공학석사학위논문

Enhanced Electrochemical Properties of Electrolytes with Nitrile-Functionalized Zwitterions for Lithium-Ion Batteries

니트릴 관능기를 포함하는 양쪽성이온을 이용한

리튬이온전지용 전해질의 전기화학적 특성 향상에 관한 연구

2012 년 8 월

서울대학교 대학원

재료공학부

이 범 진

Abstract

Nitrile-functionalized zwitterion such as 1-(propane nitrile)-2-methylimidazolium-3-(propyl sulfonate) (NI) is synthesized and investigated as an electrolyte additive toward the stabilization of the solid electrolyte interface (SEI) layer on the electrode surfaces and enhacement of ion conductivity, which can be crucial to improving the initial discharge capacity, C-rate performance and the cyclic performance under room temperature. The methyl-functionalized zwitterion (DM) is used as compared with NI in order to explain the effect of the nitrile group. The synthesized zwitterions were characterized by ^{1}H nuclear magnetic resonance (^{1}H–NMR), elemental analysis (EA), and fast atom bombardment mass spectrometry (FAB–MS). The 1.0 M $LiPF_6$ in EC/DEC (3/7 V/V) is used as a baseline liquid (E_0) electrolyte. Various amounts of the two types of synthesized zwitterion (0.02, 0.04, 0.08, 0.12, and 0.16 M) are added to E_0 (to produce the corresponding E_NI and E_DM). The electrolytes containing suitable contents of NI (E_NI), contrary to the electrolytes containing contents of DM (E_DM), is increased the ion conductivity to

that of E_0. The ion conductivity gradually increases with increasing NI content. The ion conductivity of electrolytes containing 0.08 M of NI reaches a maximum value of 7.64 mS/cm. From the FT−IR spectroscopy, it is concluded that nitrile group and sulfonate group interacted with Li^+ ion, so that these effects lead to enhancing lithium salt dissociation. The effects of both zwitterions on electrochemical performance are investigated via a combination of cyclic voltammetry (CV), linear sweep voltammetry (LSV), differential capacity measurements and electrochemical impedance spectroscopy (EIS). The interfacial resistance of the lithium-ion battery containing E_NI is lower than that of E_0. It is confirmed that a NI can enhance the stability of SEI layer on the graphite electrode surface. These results are attributed to the electrochemical adsorption of NI on the electrode surface during aging process, which prevent electrolytes decomposition on electrode surface. However, although the ion conductivity of electrolytes containing 0.08 M of NI examine here have higher values than electrolytes containing 0.04 M of NI, the initial discharge capacity and C-rate performance display the inverse behavior. Accordingly, the ion conductivity is not

crucial to determining the performance of the single full cell, at least over this ion conductivity range and in this system. The cell performance is found to depend significantly on the stability of the SEI layer, and one of the most stable SEI layers is produced by electrolytes containing 0.04 M of NI during the initial cycle. Therefore, we conclude that the nitrile-functionalized zwitterion (NI) is expected to be a good candidate for an additive to high performance lithium-ion batteries.

Keywords

Zwitterion, Nitrile group, Electrolyte additive, Solid electrolyte interface, Lithium ion battery

***Student Number*: 2010-23192**

CONTENTS

1. Introduction

Since 1912, lithium batteries have been researched by G.N. Lewis and Pioneers. However, lithium batteries did not commercially available until 1970 when the first non-rechargeable lithium batteries did. Lithium is the lightest of all metals, has the greatest electrochemical potential and provides the largest energy density for weight [1, 2]. However, lithium metal batteries are attempts to develop rechargeable lithium batteries failed due to lithium metal batteries short lifetime and explosion problem result from roughening and lithium dendrite growth on the lithium surface. This dendrite punctures the separator and then creates an internal short and in the worst case scenario, to explosion and fire accident. Because of such reason that the potentially instability of lithium metal, research turn direction to a non-metallic material using Li^+ ions.

Lithium-ions are lower energy density than lithium metal, lithium-ion is safe, provided certain precaution are acquired when battery charging and discharging performance. Sony firstly introduced the commercial lithium-ion battery (LIB) in the early 1990's and the release was a culmination of three decades worth of research intensely focused on lithium insertion materials. LIBs have become attractive as they provide higher energy density compared to other rechargeable systems such as lead-acid, nickel-cadmium, and nickel-metal hydride batteries as shown in Figure 1.

Since then, the sharp improvement in small portable appliances such as lap top

notebook and mobile phones have created an new market demand for compact, light-weight, rechargeable energy storage system offering high energy densities. Moreover, renewable energy storage system for day-to-night power shift and power source for electric vehicle (EV), hybrid electric vehicle (HEV), aerospace and military application are being pursued in national laboratories, universities and industry research facilities.

The LIB is composed of three primary functional components such as anode, cathode and electrolyte, for which a variety of materials may be used. Lithium intercalation or insertion materials have been widely investigated in the search for new electrode materials for use in high-voltage rechargeable batteries. Both the cathode and anode are lithium intercalation and insertion materials from/into which Li^+ ion can be reversibly extracted/ inserted. While one insertion materials, such as the commercially used layered $LiCoO_2$, serves as the cathode due to its high electrode potential (~4V versus Li), the other insertion materials, such as graphite , serves as the anode due its low electrode potential (< 1V versus Li).

The commercially used electrolyte solution composed of a lithium salt in variety organic carbonates mixture. The electrolyte for LIB should in theory be a perfect electronic insulator and mechanical separator with good ion conductivity. The electrolyte should have a large thermodynamic/electrochemical stability window. Since the electrolyte is near perfect electronic insulator, the electrons coupled to the Li^+ ions are transferred through the external circuit in the form of electrical energy. The lithium salt, such as $LiPF_6$, $LiClO_4$ and $LiBF_4$ for

electrolyte should be easy to dissolve, dissociate in organic solvent and dissociated ion should have the high mobility and anion should have internal oxidation in electrochemical at high voltage that should be considered when choosing a lithium salt [3]. The organic carbonated mixture containing ring shaped Ethylene carbonate (EC), chain type Diethyl carbonate (DEC), Ethylmethyl carbonate (EMC), and Dimethyl carbonate (DMC) are generally used for solvent of electrolyte. The physical and chemical properties of typical carbonated organic solvent are on the table 1 [4].

During the battery discharge performance, the Li^+ ions oxidation take place in the cathode surface, and then inserted into crystal structure (interaction) of the anode material through the electrolyte solution without it being consumed. At the same time the electrons move toward the electrode and flow out around the external circuit and accepted by the host to balance the reaction.

In order that should be useful cathode or anode material, they must have a high degree of lithium insertion, high electronic and lithium conductivity, and good reversible insertion/extraction capability with good structural and chemical stability to support repeated recharge [5].

The anode half reaction (with charging be forward) is:

$$LiCoO_2 - xe^- \leftrightarrow Li_{1-x}CoO_2 + xLi^+$$

The cathode half reaction (with charging be forward) is

$$C + xLi^+ + xe^- \leftrightarrow CLi_x$$

Overall reaction

$$LiCoO_2 + C \leftrightarrow Li_{1-x}CoO_2 + Li_xC$$

Generally, suitable electrolyte for LIB can be broad classified into liquid electrolyte (organic carbonate and ionic liquid) and polymer electrolyte (solid polymer electrolytes (SPE), gel polymer electrolytes (GPE) and hybrid polymer electrolytes). Organic carbonate electrolyte such as EC and DEC are generally used for solvent of electrolyte. The main components of LIB should resist the inevitable heating of batteries during high electric current flow; however, these are volatile and potentially flammable and can lead to the thermal runaway of batteries at any abuse condition. Many kind of electrolyte, such as gel polymer electrolyte, solid electrolyte and ionic liquid, have been tried to alternative organic carbonate electrolyte.

Solid polymer electrolytes (SPE) prepared by complexing/dissolving lithium salt into polymer matrix such as PEO and PPO. The high molecular weight polyethylene oxide (PEO)-based composite polymer electrolytes are focused as the best applicants for polymer matrix [5]. Although SPE have the advantage of no-leakage of electrolyte, flexible geometry besides higher energy density, those are still limits application for electrolyte due to insufficient ion conductivity in stable LIB systems. This reason is well known that Li^+ ion transport of SPE only occurs in the amorphous polymer region and is often controlled by the segmental motion of polymer chain.

Gel polymer electrolytes have liquid electrolyte (carbonates electrolytes or ionic liquid) trapped in polymer matrix and the preparation of physical and chemical cross-linked gel, thereby preventing leakage of liquid electrolytes. These materials have received attention because are not only the high conductivity, high energy density and better possibility, but these are also better possibility of geometrical variation and safety. Polymers including poly(ethylene oxide) (PEO), polyacrylonitrile (PAN), poly(methyl methacrylate) (PMMA), poly(vinylidene fluoride) (PVDF), and their copolymers such as poly(acrylonitrile-methyl methacrylate) (P(AN-MMA)) and poly(vinylidene fluoride-co-hexafluoropropylene) (P(VDF-HFP)) have been used as polymer matrixes for are suitable immobilize and transfer liquid electrolytes in matrixes.

Ionic liquids (ILs, so called room temperature ionic liquid) have been proposed to overcome organic carbonated electrolyte safety problem as alternative liquid electrolytes.

Many studies are focused on ILs due to their favorable electrochemical and physical properties, such as thermal stability, moderate ion conductivity, non-flammability, negligible volatility and a broad liquid temperature range [6]. However, most of ILs is still expensive and high viscosity, so that ILs can't alternate organic carbonate electrolyte solvent and used for additive to organic carbonate electrolyte to be reduction of cost and viscosity.

It is important to confirm that the difference between ILs and organic carbonate solvents. Organic carbonate electrolyte containing lithium salts, there are only two ions (cation and anion) that are came from the added salts. In contrast, ILs containing lithium salt, there are two ions from ILs as well as ions generated from the added salts. For example, if a lithium salt ($LiBF_4$) is added into imidazole-type (N-ethyl-N'-methyl imidazolium tetrafluoroborate ($EMIBF_4$)) ILs, both EMI^+ and Li^+ behave as cation in the salt/ILs mixture [7]. Therefore, the two cations (EMI^+ and Li^+) compete with each other during the charge-discharge performance. In this case, it is impossible to transport Li^+ selectively in salt and ILs mixture in a potential gradient, so that the competition of EMI^+ with Li^+ ions leads to decreasing the Li^+ ions transference number. Another example is Butyldimethyl-imidazolium hexafluorophosphate ($BDMIPF_6$) added electrolytes which are composed of PC and $LiPF_6$ 1M. During the charge-discharge, $BDMI^+$ and Li^+ two cations compete against each other under potential gradient [8]. Thus the $BDMI^+$ forms a blocking layer around the electrodes, resulting in deceasing performance.

The workers have been trying to solve the ILs problem of which is the migration of ILs ions under potential gradient. Dr. Masahiro Yoshizawa et al. proposed a simple and brilliant idea, namely, covalently immobilized of both cationic unit and anionic one on same molecular [9]. These salts called “zwitterions” as shown in Figure 3. The zwitterions are expected to stationary under potential gradient, and these are showing little migration under potential gradient because they have a zero net charge. Moreover, use of a zwitterion as a dissociation enhancer in combination with the lithium salts results in single ion electrolytes, so that these electrolytes showed ions conductivity of 10^{-5} – 10^{-7} S/cm at room temperature. Moreover, it is also founded that the rate capability of asymmetrical lithium cell is enhanced by adding zwitterion in electrolytes due to formation of the low resistance solid electrolyte interface layer (SEI layer) [10]. Because these advantages are affected by the structural characteristics of the zwitterion, many researchers have attempted to synthesize a variety of molecular zwitterion structures. The Table 2 summarizes structure and thermal property of previously prepared zwitterions. However, the electrochemical stability of positive charge site on zwitterion is not sufficient for the reversible charge–discharge so that zwitterion decomposed on the electrode surface. This problem is results in reducing stability of the SEI layer and results in low cyclic performance and C-rate performance. Therefore, the improved electrochemical stability of positive charge site of zwitterion is necessary.

Since this problem is affected by molecular structure of the zwitterion, the design

of molecules for enhanced electrochemical stability is an important part. There are several kinds of structure parameters that affect the electrochemical properties, such as anion and cation site, structure and chain length of spacer between anion and cation. Particularly, the characteristic of anion site is very important because anion site have to interact with Li^+ ion. Dr. Asako Narita [10] elucidated the effect of these three parts on the characteristics of the zwitterions. She determined that electrolytes containing sulfonate or Bis(sulfonyl)imide anion type zwitterion are relatively high Li^+ ion transport. She concluded the most appropriate cation structure by comparing with several zwitterions containing different cation site. These results indicate that cation structures like typical ILs, such as N-methylpyrrolidinio-sites and TFSI anions, are not always effective for improving ion conductivity of electrolytes containing zwitterion and lithium salt mixture. In this reason, N-ethylimidazolio group was recommended by the one of the most appropriate cation site. And, the last factor of alkyl chain (spacer) length between the cation was determined to be 4 to 7 CH_2 units. Therefore, these properties can be utilized to design new molecular.

Recently, many workers have been tried to synthesize of the diverse molecular zwitterion structure. For instance, the introduction of long alkyl chains in cation site is possible to make zwitterion with a low T_m, but the introduction of long alkyl chains accompanied by lower ion density and increases viscosity [11]. Another example is the various types of multi-functional zwitterions. These are expected that the favorable interaction between functional group and Li^+ ions could enhance electrochemical properties

of electrolytes. For example, introducing both functional group (ester, ether group) and sulfonate group on the imidazole ring, it can obtain more enhanced electrochemical property than zwitterions having alkyl chains and sulfonate groups [12−14]. Hence, it is possible that enhancement of electrochemical properties can be obtained by introduction of different functional group on zwitterion structure.

A nitrile (interchangeably by the cyano in industrial literature) is any organic that which has a polar carbon and nitrogen triple bond group. A nitrile group which is composed of carbon and nitrile strongly polarized towards nitrogen due to the difference in the electronegativity between the carbon =2.55 and the nitrogen = 3.04. Hence, molecular dipole moments (negative charge) can be high. These characterizations were used for LIB electrolytes. For example, polyacrylonitrile (PAN) base gel polymer electrolytes exhibit ion conductivity ranging from 10^{-4} to 10^{-3} S/cm at room temperature, which is near to that of commercial electrolytes, because interaction between the Li^{+} and the nitrile group of PAN promote dissociation of lithium salt [15, 16]. The nitrile group is not only the effect of the structural formula of polymer matrix but also the effect of the molecular structure of the ionic liquid on electrochemical properties. Introducing nitrile group on ILs was use as the electrolytes [17, 18]. The nitrile-functionalized ILs show enhanced the cathodic stability and improved cyclic performance due to formation of the stable solid electrolytes interface (SEI) layer. Therefore, it was postulated that the presence of nitrile groups on a zwitterion could yield similar effects.

This study introduced nitrile functional groups onto zwitterions based on an imidazolium ring to synthesize highly electrochemically stable zwitterions. The influence of the nitrile functional zwitterion on LIB performance was examined. These imidazole based zwitterion consist of nitrile group at 1-C position, methyl group at 2-C position and sulfopropyl at 3-C position on the imidazolium ring as shown in Figure 4. The nitrile-functionalized zwitterion is expected to promote stability of positive charge site, which electrochemically absorb on electrode surface and suppress the decomposition of the electrolytes on the electrode surface, as shown in Figure 5. Furthermore, the functionalized nitrile group is also expected to dissociation of the lithium salts. Because the nitrile group can straightly interact of Li^+ ion, it can be cooperated with sulfonate group in dissociation of the lithium salts, as shown in Figure 6. The synthesized zwitterion was characterized by ^1H nuclear magnetic resonance (^1H–NMR), elemental analysis (EA) and fast atom bombardment mass spectrometry (FAB–MS), respectively. The thermal properties were determined by thermo gravimetric analysis (TGA) and differential scanning calorimetry (DSC). The electrolytes were prepared by mixing the zwitterions and the organic carbonate electrolytes. The ion conductivity is estimated by electrochemical impedance spectroscopy (EIS). In addition, the interaction of lithium salt and functional groups has been investigated by means of Fourier–Transform Infrared (FT–IR) spectra. The interfacial reaction between electrode and electrolytes were obtained by linear sweep voltammetry (LSV) and cyclic voltammetry (CV). Finally, a cell performance test was conducted using a

single full cell (SFC).

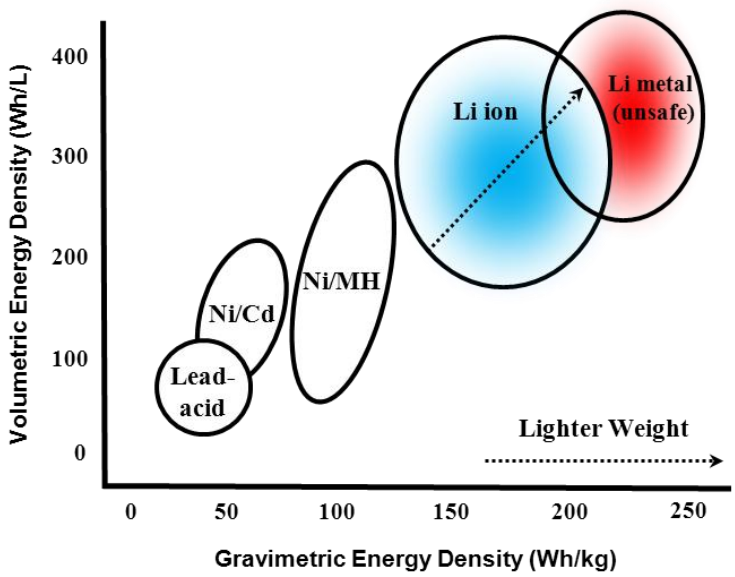

Figure 1. Comparison of the energy densities of different battery systems

Table 1. Structure and properties of some solvents used for LIB electrolytes

Solvent name	structure	melting point (℃)	boiling point (℃)	Dielectric constant (40℃)
Ethylene Carbonate (EC)		39	248	89.6
Propylene Carbonate (PC)		-49	240	64.4
Dimethyl Carbonate (DMC)		4.6	91	3.12
Diethyl Carbonate (DEC)	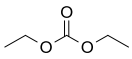	-43	126	2.82
2-methyl-tetra-hydrofuran (2-MeTHF)		-137	79	6.29
γ- Butyro lactone (GBL)		-43	204	39.1

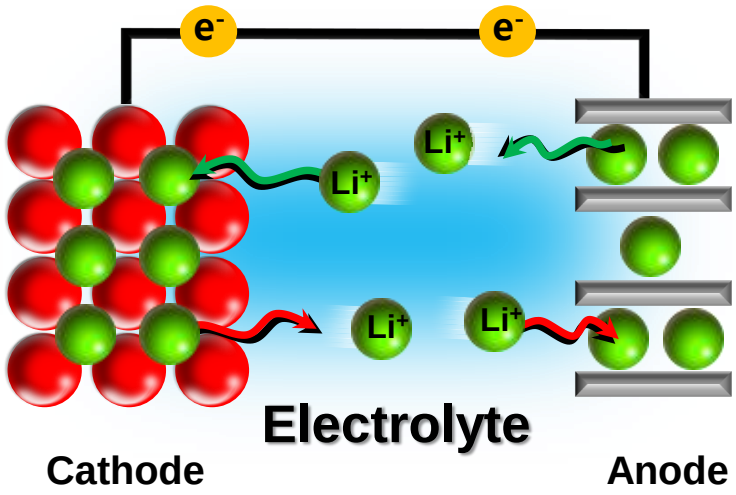

Figure 2. General layouts of a LIB and the charge-discharge process

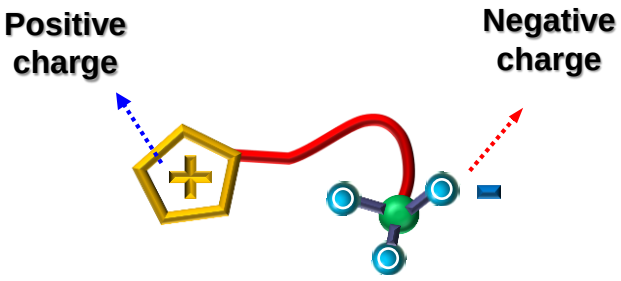

Figure 3. Zwitterion immobilized cationic and anionic charges on the same molecule

Table 2. Summarizes structure and thermal property of various zwitterions

Zwitterion structure	Melting point (℃)
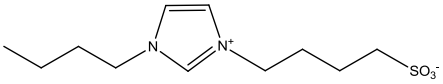	158
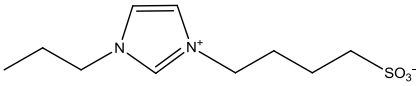	158
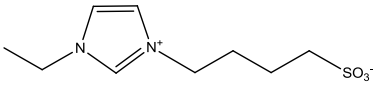	206
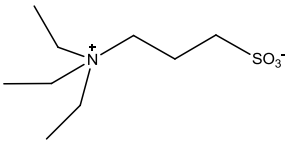	285
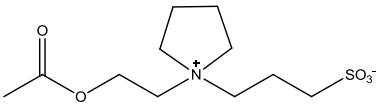	174
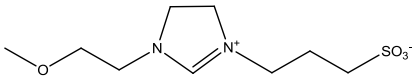	175

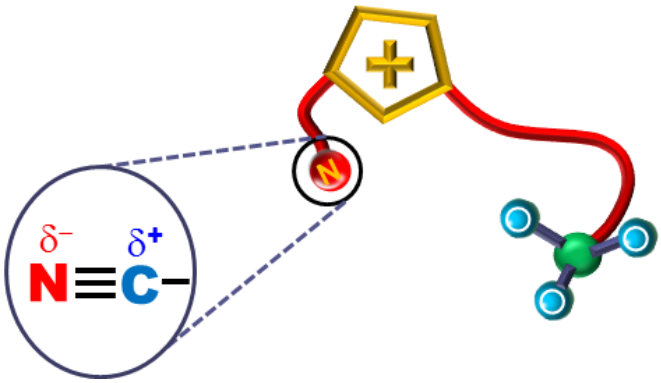

Figure 4. Schematic diagrams of nitrile-functionalized zwitterion

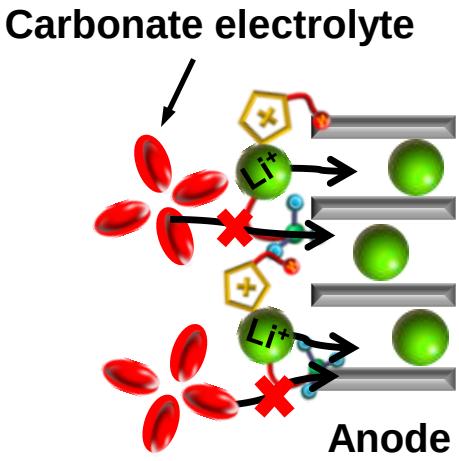

Figure 5. Schematic diagram of formation SEI layer on electrode surface

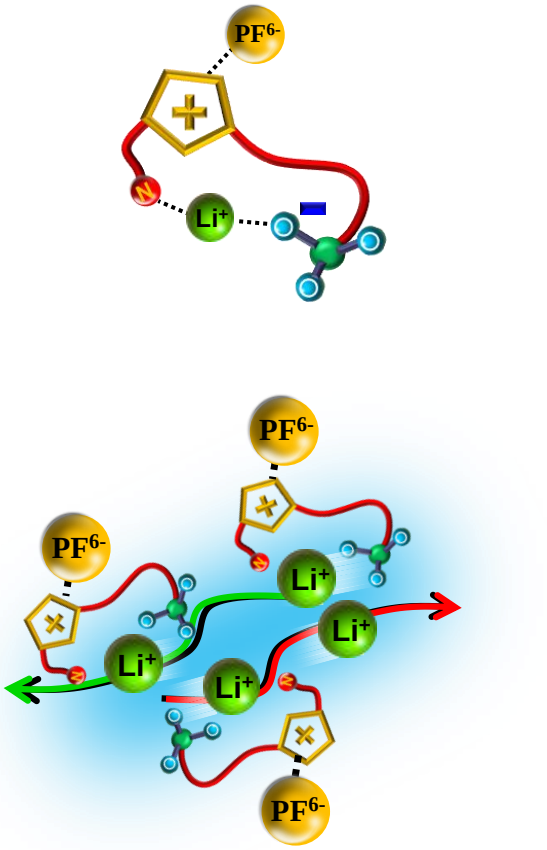

Figure 6. Schematic diagram of dissociation of Li^+ ion by nitrile-functionalized zwitterion

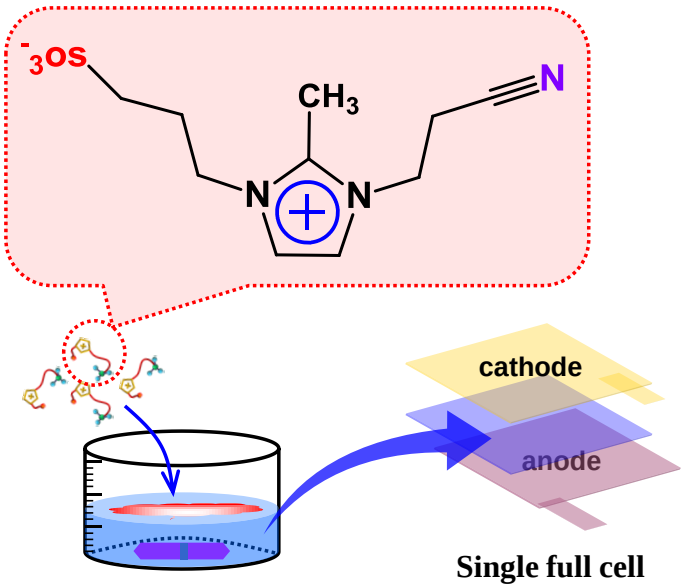

Figure 7. Schematic diagram of preparation of electrolytes mixture and single full cell

2. Experimental Section

2.1. Materials

1-(2-Cyano ethyl)-2-methylimidazole (97%, TCI) and 1, 2- Dimethyl-1H-imidazole (98%, Aldrich) were used as precursor for synthesizing of two kind of zwitterion. 1, 3-Propanesultone (99%, Aldrich) was used as synthesizing for zwitterion anion site. *N*, *N*-dimethylformamide (DMF) (99.9%, Junsei), Acetone (99.9% Junsei) were used for solvent which were distilled over appropriate drying agents prior to use.

Battery-grade ethylene carbonate (EC), diethyl carbonate (DEC), and $LiPF_6$ (99.99%, battery grade, Aldrich) were used without further purification. Graphite and $LiCoO_2$ electrodes were received from Enerland Co. as the mass-producing grade of Li-ion battery. The electrolytes systems were prepared in the 1 M $LiPF_6$ in EC/DEC (3/7 v/v).

2.2. Preparation of the zwitterion

The two kinds of imidazolium zwitterion were prepared by nucleophilic ring-opening reactions, the first of which consisted of nitrile group at 1-C position, methyl group at 2-C position and sulfopropyl at 3-C position on the imidazolium ring (hereafter referred to NI), and second of which consisted of methyl group at 1-C and 2-C position and sulfopropyl at 3-C position on the imidazolium ring (hereafter referred to DM). These two

kinds of zwitterion synthetic scheme were shown in Figure 9.

2.2.1. Synthesis of nitrile functionalized zwitterion (NI)

Firstly, DMF, solvent, was degassed for 1h. 1-(2-Cyano ethyl)-2-methylimidazole (50 mmol) was dissolved in degassed DMF (50 ml) and stirred for 2h. 1, 3-Propanesultone (55 mmol) was added slowly dropwise at 80 ℃ and reacted for overnight at reflux with a vigorous stirring. Then the white precipitates collected, washed with DMF several times, dried under vacuum. These NI are store in a glove-box due to hygroscopic.

2.2.2. Synthesis of nitrile methyl functionalized zwitterion (DM)

Firstly, Acetone, solvent, was degassed for 1h. 1, 2- Dimethyl-1H-imidazole (50 mmol) was dissolved in degassed acetone (50 ml) and stirred for 2h. 1, 3-Propanesultone (55 mmol) was added slowly dropwise at room temperature and reacted for 8 hour at reflux with a vigorous stirring. Then the white precipitates collected, washed with acetone several times, dried under vacuum. These DM are also store in a glove-box.

2.4. Preparation of electrolytes mixture and ion conductivity test

The 1.0 mol/L $LiPF_6$ in EC/DEC (3/7) was used as baseline liquid (E_0) electrolytes as shown in Figure 8. Various amounts of the two types of synthesized zwitterion (0.02, 0.04, 0.08, 0.12, and 0.16 M) were added to E_0 (to produce the corresponding E_NI and E_DM). The mixed electrolytes were dissolved by vigorous stirring for 24h. Electrolytes formulation was performed under an argon atmosphere in a glove box whose humidity was controlled below 10 ppm. As shown in Table 3, there is the sample code of resulting electrolytes mixtures.

2.5. Fabrication of single full cell

All the experiments were performed using 3 × 3 cm^2 homemade pouch single full cells as shown in Figure 9. All the single full cells were composed of graphite (synthetic graphite) and $LiCoO_2$, which were received from Enerland Co. as mass production grade for Li ion battery. Each electrode was dried for 12 hr at 80 ℃ in a vacuum oven before the cell fabrication. Celgard 3051 was used as a separator. The entire single full cell system was assembled in the glove box filled with argon gas, whose humidity was controlled below 10 ppm.

2.6. Characterization

2.6.1. Identification of the zwitterion formation

The structure of all synthesized NI and DM was performed by ^{1}H Nuclear magnetic resonance (^{1}H–NMR) spectroscopy employing a Buker Avance 600 MHz spectrometer with the tetramethylsilane (TMS) proton signal as an internal standard in deuterium oxide (D_2O). The molecular weight of NI and DM was confirmed by fast atom bombardment mass spectrometry (FAB–MS) employing a Jeol JMS-700 high resolution mass spectrometer. The elemental analysis (EA) was carried out using CE instruments EA 1112 elemental analyzer to determine the C, N, H and S atom contents of the NI and DM.

The thermal properties of NI and DM was analyzed by dynamic scanning calorimeters (DSC) and thermal gravimetric analyzer (TGA) with and TA Instruments Q500 under heating rate 10 ℃/ min from 25 to 500 ℃ in N_2 and TA Instruments 2920 under heating rate 5 ℃ / min from 0 to 260 ℃, in N_2

2.6.2. Ion conductivity test

The conductivities of the NI and DM incorporated electrolytes at different weight ratio and temperature were confirmed by electrochemical impedance (EIS, frequency from 100 kHz to 1 kHz) using an Solartron 1255. For this test, stainless still (SS) disc cell was assembled as Figure 10 and kept at thermo hydrostat incubator for constant temperature.

The interaction between functional group in zwitterion and Li^+ ion was measured Fourier-Transform Infrared (FT–IR) spectra on a Perkin Elmer GX spectrophotometer.

2.6.3. Interfacial reaction between electrode and electrolytes

The electrochemical stability for electrolytes mixtures were evaluated by linear sweep voltammetry (LSV) with a scan rate 5 mV s^{-1} at 20 ℃ , which were carried out using a scanning electrochemical microscopy (SECM, CHI900B, CH Instruments, USA) in the glove box. As for the working electrode, platinum (Pt, d = 0.2 cm) was used and as for the counter and reference electrode the lithium metal was used. Before the LSV measurement, the Pt was polished on diamond slurry (15 m, BASI). Cyclic voltammetry (CV) was performed on graphite negative electrode in a range from 3.0 V to 0.0 V (vs. Li/Li^+) with 0.05 mV/s. LSV and CV are performed with using a beaker-type electrochemical cell.

2.6.4. Single full cell performance test

The open circuit voltage (OCV) was checked using a battery cycler (WBCS3000, Wonatech) for 2 hr. Then the SFCs were charged from OCV to 4.2 V at 0.2 C rate, followed by a constant voltage (4.2 V) to 0.02 C capacity drop (CC–CV charging), and were discharged to 2.75 V at 0.2 C (CC discharging), and SFCs were charged to 4.2 V at 0.2 C,

and then discharged to 2.75 V with different C rate (0.2, 0.5, 1.0 and 2.0 C) to investigate the rate performance. Finally, all SFCs were cycled with 1.0 C rate charge and discharge at 100th. The resistance of SFCs was measured by AC impedance analyzer with frequency range from 200 KHz to 10 mHz at 4.2 V (Li/Li^+). The obtained impedance data were analyzed using the Zman ver. 2.0 software.

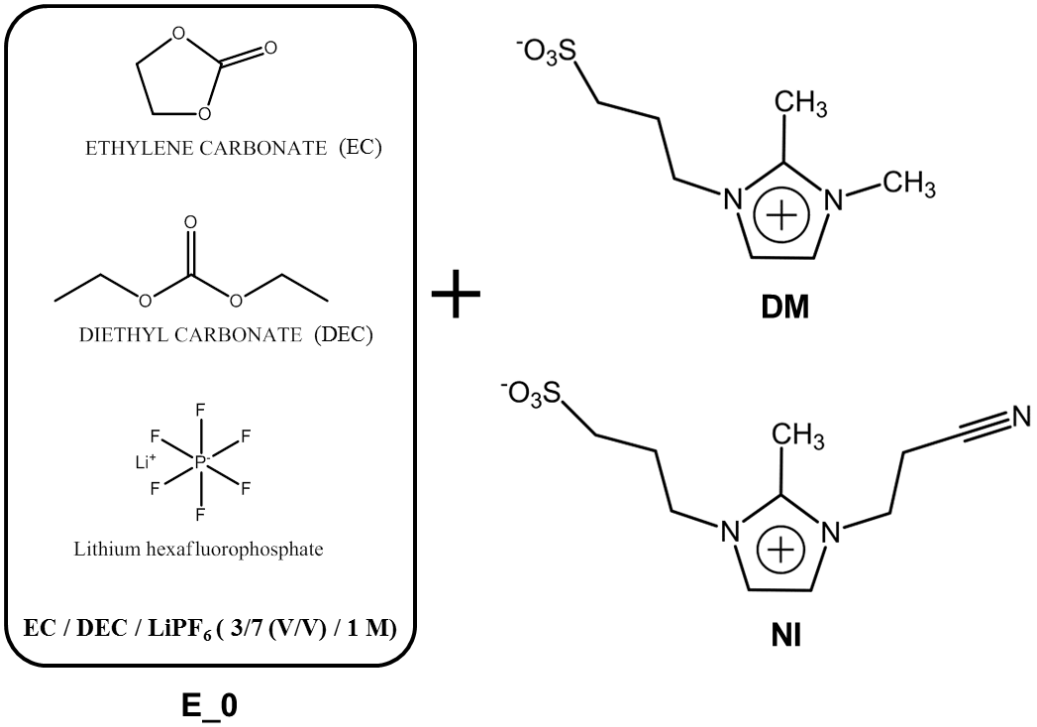

Figure 8. Preparation of electrolytes mixture

Sample	Content of zwitterion (M)	Sample code
EC/DEC/$LiPF_6$ (3/7 (V/V)/ 1 M)	0.00	E_0
E_0 + NI	0.02	E_NI 2
	0.04	E_NI 4
	0.08	E_NI 8
	0.12	E_NI 12
	0.16	E_NI 16
E_0 + DM	0.02	E_DM 2
	0.04	E_DM 4
	0.08	E_DM 8
	0.12	E_DM 12
	0.16	E_DM 16

Table 3. Formulation of electrolytes mixture

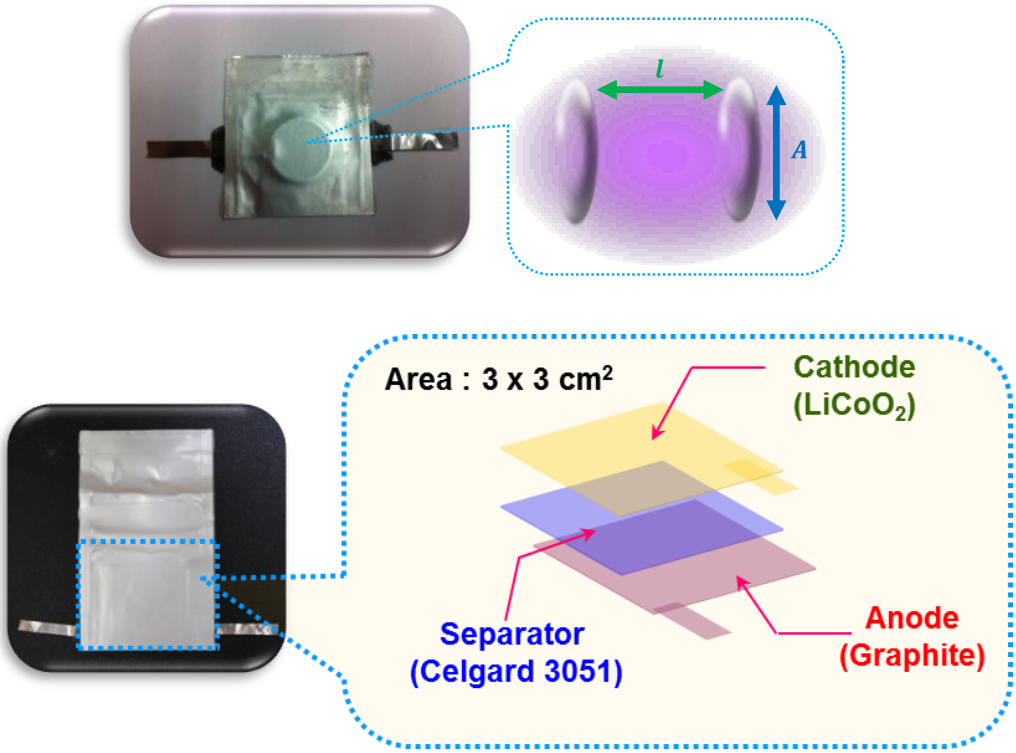

Figure 9. Stainless still (SS) disc cell and Single full cell (SFC) with graphite/ $LiCoO_2$ electrode

3. Results and Discussion

3.1. Synthesis of 1-(propane nitrile)-2-methylimidazolium-3-(propyl sulfonate) (NI)

The 600MHz ^{1}H nuclear magnetic resonance (^{1}H–NMR) spectra of 1-(2-Cyano ethyl)-2-methylimidazole (Pre-NI) and 1-(propane nitrile)-2-methylimidazolium-3-(propyl sulfonate) (NI) is shown in Figure 12. The nucleophilic attack of the Pre-NI (1-H singlet at 7.14 ppm, 2-H singlet at 6.92 ppm, 3-H singlet at 2.39 ppm, a-H triplet at 4.29 ppm and b-H triplet at 2.98 ppm) nitrogen occurs at the carbon of propanesultone. The all NMR spectrum of synthesized NI (1-H doublet at 7.56 ppm, 2-H doublet at 7.55 ppm, 3-H singlet at 2.39 ppm, 4-H triplet at 4.34 ppm, 5-H quintet at 2.73, 6-H triplet at 2.97, a-H triplet at 4.54 ppm and b-H triplet at 3.13 ppm, as shown in Table 4) shifted downfield due to positive charge indication of imidazole ring on NI. Particularly, the 1 and 2 peaks which are signals of NCH_2 in hetero aromatic in Pre-NI appear to 7.14 and 6.92 ppm. However, because NI indicated a symmetrical structure, these are so overlap each other (7.56 ppm and 7.55 ppm), and look like a doublet. This results show that NI is clearly synthesized by nucleophilic ring-opening reactions. The value of degree of substitution (DS) was determined by Elemental analysis (EA). The stoichiometry of NI was derived from the EA are shown in Table 5. From the results of the EA, the value of Degree of substitution (DS) was found to be approximately 0.98. These results mean that Pre-NI is successfully

conversion of NI. The Fast atom bombardment mass spectroscopy (FAB–MS) is excellent in giving the correct molecular formula. In shown Figure 13, it can be seen that the major peaks (258 m/z : [M + H]$^{+}$, 176 m/z : [M – SO_3^- - H]$^{-}$, 162 m/z : [M – $CH_2SO_3^-$ – H]$^{-}$, 149 m/z : [M – $CH_2CH_2CH_2SO_3^-$ + H]$^{+}$, 136 m/z : [M – $CH_2CH_2CH_2SO_3^-$ + H]$^{+}$ and 95 m/z : [M – $CH_2CH_2SO_3^-$ + H]$^{+}$). Overall, ^{1}H-NMR, EA and FAB-MS results can be successfully achieved with the confirmation of synthesized NI.

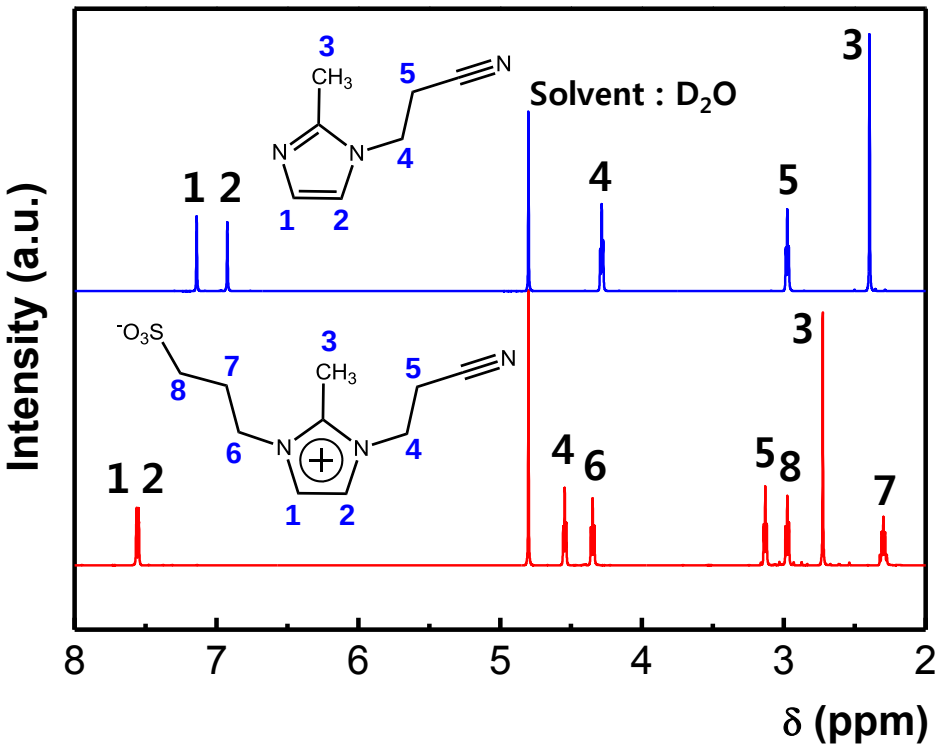

Figure 10. 1H−NMR spectrum of NI

Table 4. The interpretation of the $^{1}H-NMR$ spectrum of NI

Region		split	Relative integral	Region		split	Relative integral
1	NCH	d	1.91	**5**	CH_2	t	2.02
2	NCH	d		**6**	NCH_2	t	2.07
3	CH_3	s	3.0	**7**	CH_2	q	2.10
4	NCH_2	t	1.99	**8**	CH_2S	t	2.16

*S : Singlet *t : triplet *d : doublet *q : quintet

Table 5. Elemental analysis of NI

Element	C	N	H	S
Weight percentage (%)	46.88	16.34	6.04	12.36
Atomic weight	12.01	14.00	1.00	32.00
Number ratio	**10.06**	**3.03**	**15.68**	**1.00**
Target number ratio	**10**	**3**	**15**	**1**

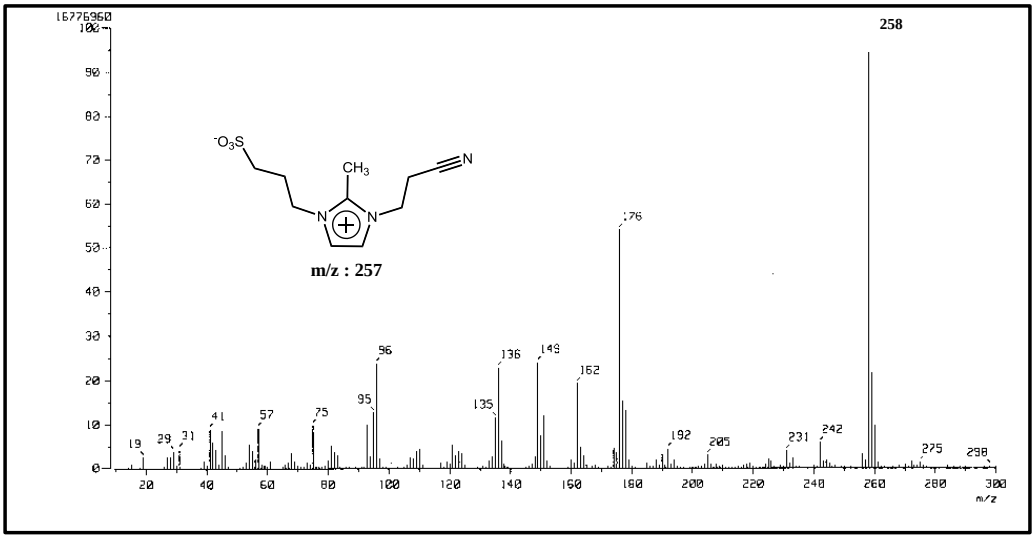

Figure 11. FAB–MS spectrum of NI

3.2. Synthesis of 1,2-dimethylimidazolium-3-(propyl sulfonate) (DM)

The 600MHz $^{1}H-NMR$ spectra of 1,2-Dimethylimidazole (Pre-DM) and 1,2-dimethylimidazolium-3-(propyl sulfonate) (DM) which are comparison group with NI is shown in Figure 14. It is also nucleophilic attack of the Pre- DM (1-H doublet at 6.82 ppm, 2-H singlet at 6.71 ppm, 3-H singlet at 2.18 ppm and a-H triplet at 3.41 ppm) nitrogen occurs at the carbon of propanesultone. The all NMR spectrum of synthesized DM (1-H doublet at 7.41 ppm, 2-H doublet at 7.34 ppm, 3-H singlet at 2.61 ppm, 4-H triplet at 4.29 ppm, 5-H quintet at 2.26, 6-H triplet at 2.95 ppm and a-H singlet at 3.77 ppm, as shown in Table 6) shifted downfield due to similar effects of positive charge indication on NI. In comparison with NI, because DM indicated an asymmetrical structure, the 1 and 2 peaks (7.41 ppm and 7.34 ppm) which are signals of NCH_2 in hetero aromatic in DM are obviously indicated in each chemical shift. This results show that DM is clearly synthesized. The value of DS was determined by EA. The stoichiometry of DM was derived from the EA are shown in Table 7. From the results of the EA, The value of DS was found to be approximately 1.00. These results mean that Pre-DM is successfully conversion of DM. The FAB–MS is excellent in giving the correct molecular formula. In shown Table 5, it can be seen that the major peaks (219 m/z : $[M + H]^{+}$, 137 m/z : $[M - SO_3^{-} - H]^{-}$, 123 m/z : $[M - CH_3SO_3^{-}]^{+}$, 110 m/z : $[M - CH_2CH_2SO_3^{-} + H]^{+}$). Overall, $^{1}H-NMR$, EA and FAB−MS results can be successfully achieved with the confirmation of synthesized DM.

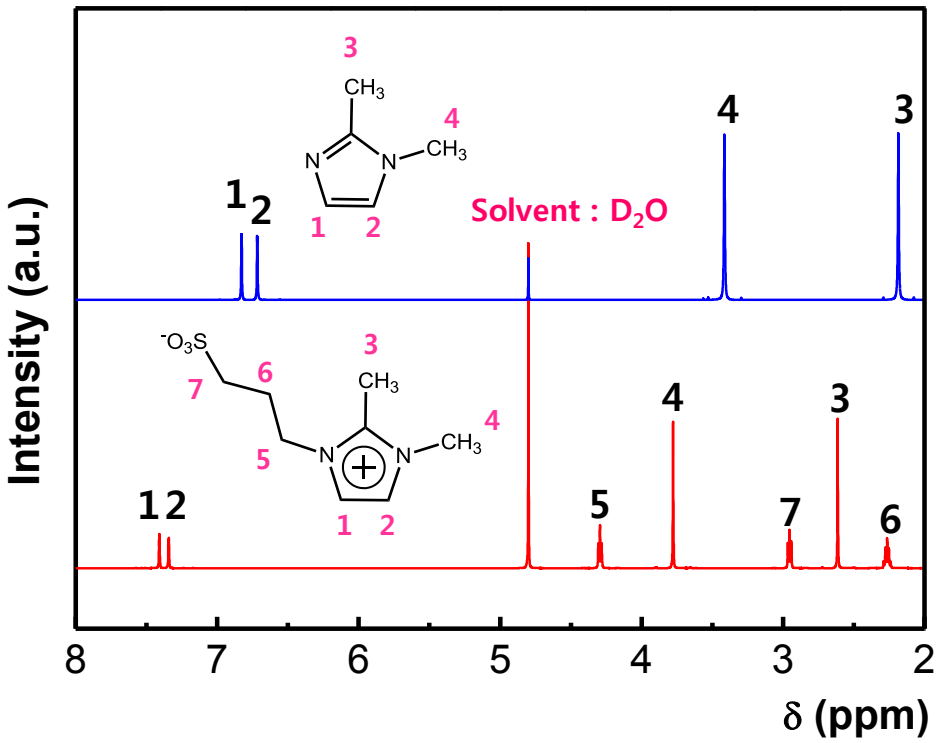

Figure 12. ^{1}H−NMR spectrum of DM

Table 6. The interpretation of the $^{1}H-NMR$ spectrum of DM

Region		split	Relative integral	Region		split	Relative integral
1	NCH	d	1.00	5	NCH_2	t	2.20
2	NCH	d	0.98	6	CH_2	t	2.19
3	CH_3	s	3.21	7	CH_2S	t	2.23
4	NCH_3	s	3.22				

Table 7. Elemental analysis of DM

Element	C	N	H	S
Weight percentage (%)	43.89	12.83	6.66	14.65
Atomic weight	12.01	14.00	1.00	32.00
Number ratio	7.97	2.02	14.63	1.00
Target number ratio	8	2	14	1

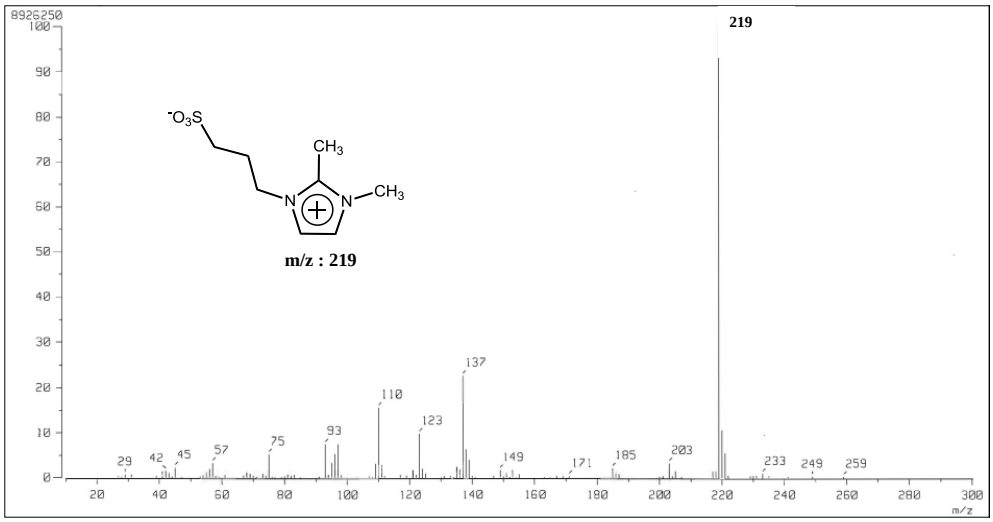

Figure 13. FAB–MS spectrum of DM

3.3. Thermal properties

The thermal stabilities and thermal properties of the zwitterion were examined by TGA and DSC, respectively. Figure 15 illustrate the DSC diagrams of the zwitterions on their second heating trace (10 ℃ min^{-1}). The phase properties of NI and DM were examined, including the crystallization point (T_c), the melting point (T_m), and the glass transition temperature (T_g). The DSC curves during the first heating scan of the zwitterion indicated T_m values of 237 ℃ (NI) and 240 ℃ (DM); however, during the second heating scan, the DM displayed one exothermic peak and two endothermic peaks. The DM showed an endothermic peak prior to melting, which suggested that the crystal was transformed into a different crystalline form. On the other hand, the NI only displayed a T_g during the second scan. The nitrile group includes strongly electron-withdrawing groups. This functional group can change the electron distribution over the whole zwitterion molecular system. Accordingly, although introducing alkyl chains may be effective in reducing the crystallinity of the zwitterions, the biased electron distribution in NI compared with DM made it more difficult to form crystalline structures. Moreover, because the NI decomposed prior to melting, the melting temperature was superseded by the decomposition temperature of the zwitterion, as shown in Figure 16. A comparison of these two zwitterions showed that DM displayed a weight loss region, whereas NI displayed two distinct stability regions. The initial weight loss of NI occurred around 24% in the temperature range 220–250 ℃,

which was likely attributed to the nitrile functional group. Only a small degree of weight loss was displayed in DM at 110 ℃ due to the solvate or hydrate. As a result, the NI exhibited a high thermal stability, and the LIB electrolytes containing this zwitterion were expected to be safe, even at high temperatures.

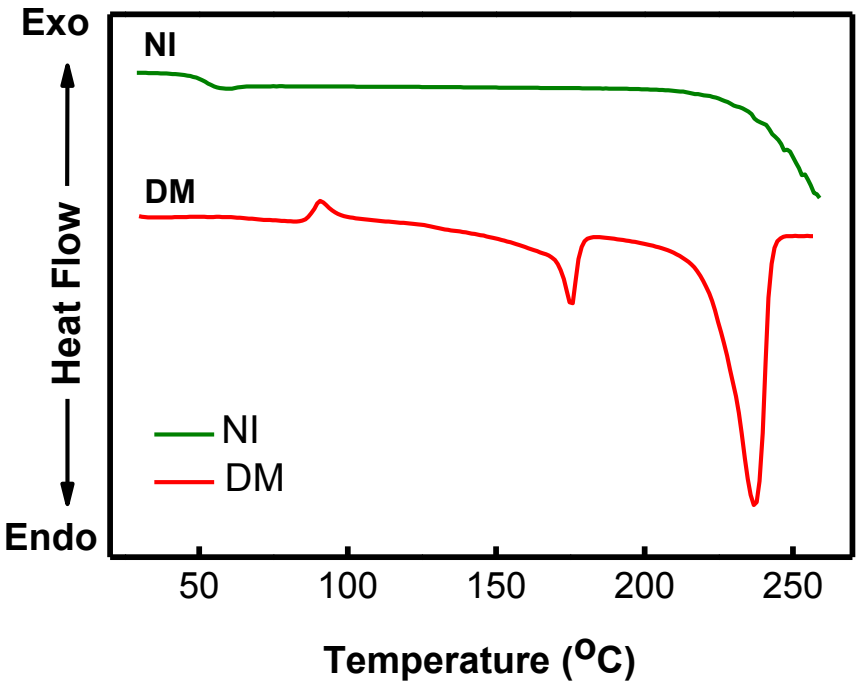

Figure 14. DSC diagram of NI and DM zwitterion

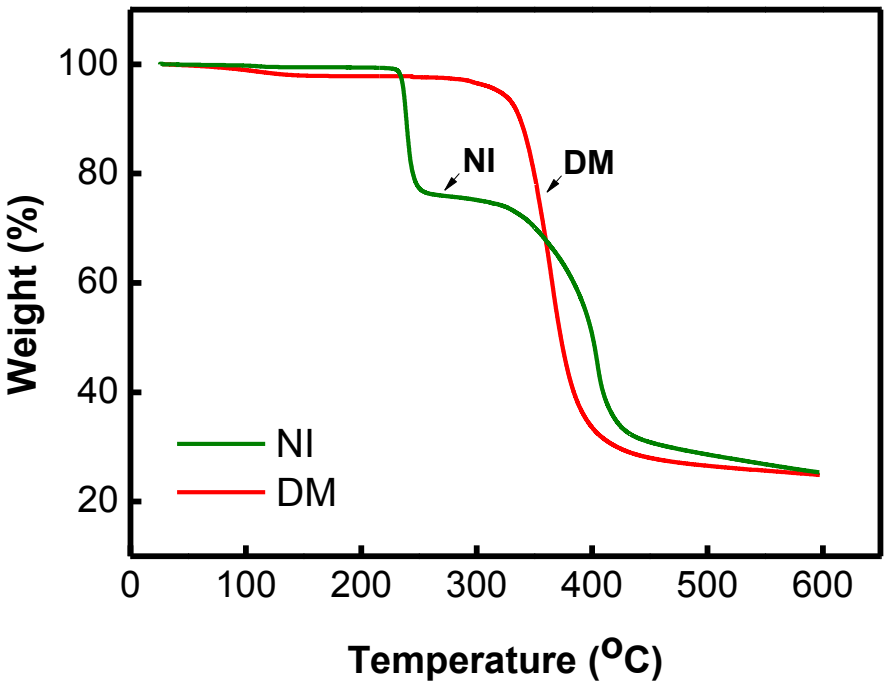

Figure 15. TGA diagram of NI and DM zwitterion

3.4. Electrochemical Analysis of Electrolytes

3.4.1. Ion conductivity test

The ion conductivity reflects of the total charge on each species of the electrolytes. Because a high ionic conductivity is associated with a low ohmic potential loss, the high ion conductivity is an essential requirement for electrolytes. The room temperature (20 ℃) ion conductivities of samples which incorporated with various amounts of each zwitterion are shown in Figure 18 and which calculated by using the bulk electrolytes resistance (R_b) according to the following equation:

$$\sigma = \frac{L}{R_b \cdot A}$$

where A is the contact area between stainless steel electrode and the electrolytes and L is the thickness between two SS. The bulk resistance, R_b, was obtained from the impedance data. The calculated ion conductivity of E_0 can approach the similar value as compared to reference paper [19, 20]. The ion conductivity of the NI added electrolytes increases gradually at low concentration. Ion conductivity of E_NI 8 reaches the maximum value, 7.64 $mS \cdot cm^{-1}$. When the NI concentration is more than the E_NI 8, the ion conductivity is gradually decreased. Therefore, the E_NI 8 was considered the highest conducting

electrolytes. In contrast, when the DM added into E_0, ion conductivity gradually reduces the increasing the DM concentration. This is explained by assuming that the functionalized nitrile group is cooperated with sulfonate group in dissociation of Li^+ from the salts, thus causing a decrease in the interaction between Li^+ and the PF_6^-, followed by a decrease in viscosity and an increase in Li^+ ion mobility. However, if excessive the NI is mixed with the electrolytes, Li^+ will be surrounded by a large number of nitrile group or SO_3^- forming ionic atmosphere; therefore Li^+ are trapped in the ionic atmosphere and increasing viscosity results in decreasing ion conductivity [21]. Almost all of the most commonly studied that the ion conductivity of an organic carbonates base electrolytes decreases by addition of ILs or additives, because of the increase of the viscosity [22, 23]. Thus the DM mixed electrolytes is corresponded to this case. Figure 19 illustrated of temperature dependence of ion conductivities electrolytes which are consisted with the E_0, the E_NI 8 and the E_DM 8. Overall, the ion conductivity was found to increase with increasing temperatures in the range. The conductivity of the E_NI 8 is higher than that of the E_0 and the E_DM 8 at the same temperature.

The interaction between Li^+ ions and zwitterion was investigated by FT−IR spectroscopy. The Figure 20 illustrates of FT−IR spectra of zwitterion and $LiPF_6$ mixtures. The peak of 2250 cm^{-1} at (C) that associated with the bearing nitrile group at NI shifted to the high frequency at 2258 cm^{-1} when mixed with 1.0 equiv. of $LiPF_6$. It is suggested that lithium salts were solubilized with the support of interaction between nitrile group and Li^+

ion. Furthermore, the peak of 1039 cm^{-1} that assigned to the double bond of the sulfonate group moved to the 1051 cm^{-1}. In comparison with the DM, the NI is stronger interaction between Li^+ and sulfonate group than the DM. Therefore, FT−IR spectra with NI and DM demonstrate that Li^+ ion interacts with both nitrile and sulfonate group, thereby NI is facilitating Li^+ dissociation.

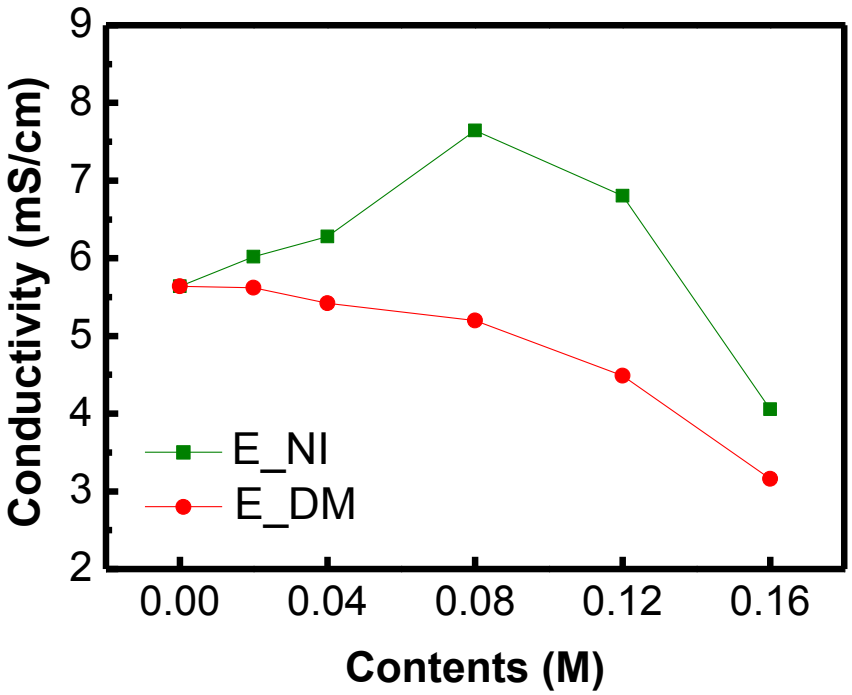

Figure 16. Variation of conductivity with zwitterion concentration

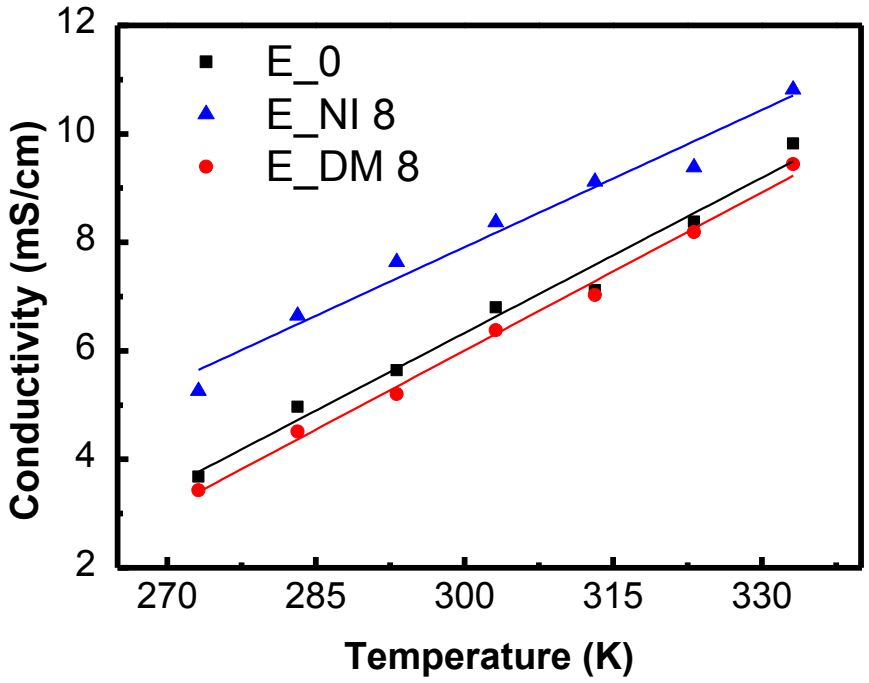

Figure 17. Temperature dependence on ion conductivities of electrolytes containing 0.08 M zwitterion

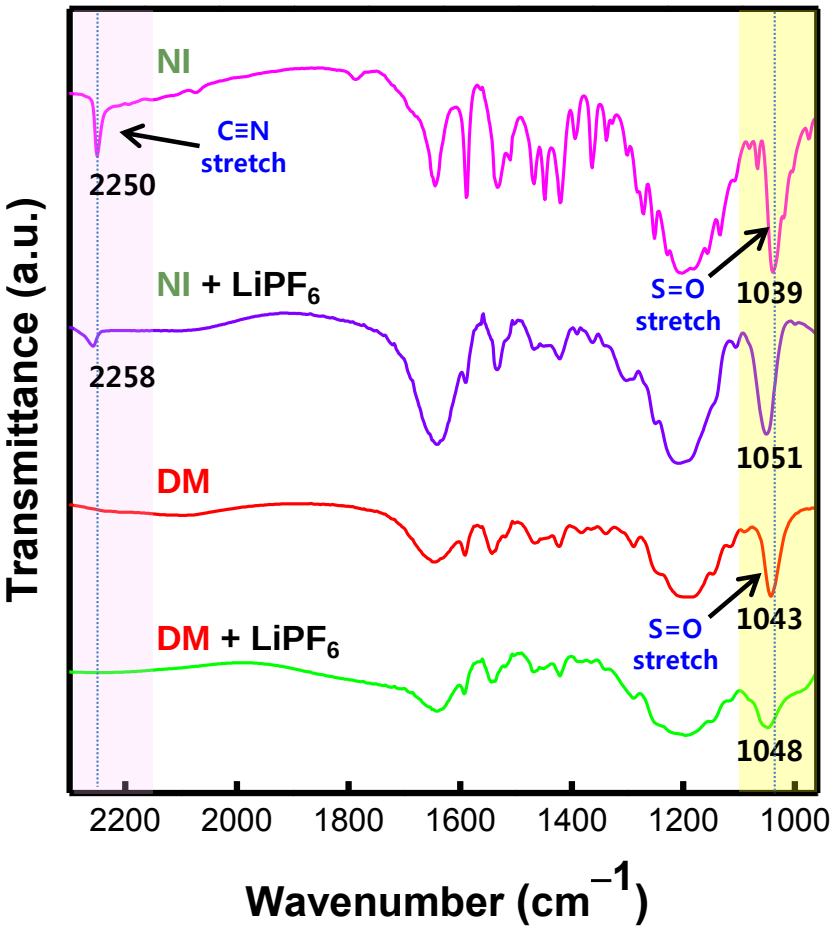

Figure 18. FT−IR spectra of interaction between zwitterion and $LiPF_6$; NI, NI+ $LiPF_6$, DM, DM+$LiPF_6$

3.4.2. Interfacial reaction between electrode and electrolytes

The electrochemical stability of the electrolytes was determined by linear sweep voltammetry (LSV). This was performed with counter and reference electrode of lithium metal and working electrode of platinum (Pt) at a scanning rate of 5.0 mV/s. In the Figure 19 of E_0, the two reduction peaks are observed between 2.0 V and 3.2 V which related with the reduction of the EC and DEC [24]. In case of the E_NI 4 and the E_DM 4, they show three reduction peaks which are associated with decomposition of containing electrolytes and zwitterion. These three electrolytes show difference of reduction current intensity. Comparing the E_NI 4 with the E_0, the E_NI 4 has the lower reduction current than the E_0. These low-intensity current mean that electrolytes reduced the reduction decomposition on the electrode surface. In other words, NI prevented the electrolytes decomposition on the electrode surface. Otherwise, the E_DM 4 has higher current intensity compared to the E_0. Therefore, LSV indicated that The NI was inferred to prevent electrolyte decomposition on the electrode surface.

The zwitterion compounds affected the compatibility between the graphite anode and the electrolytes, as further investigated by cyclic voltammograms (CV). The CV of E_0, E_NI 4 and E_DM 4 are shown in Figure 20. Graphite electrodes, three cycles, a scan rate of 0.5 mV/s, and a voltage range of 0–3 V (versus Li/Li^+) were used. As shown in Figure 20 (a), the E_0 has several redox peaks in the first cycle. The broad intense reduction peak

indicated between around 0.7 V and 0.5 V, corresponding to the reduction of the EC. The reduction at 0 V and the oxidation at around 0.6 V related to lithium intercalation/deintercalation at the graphite layers [25]. The reduction peak of EC is disappeared in the second scan, which is effected by formation of the SEI layer on the graphite electrode preventing the further decomposition of electrolytes. As shown in Figure 20 (b), E_NI 4 displayed several redox peaks at 0.5 V, 0 V, and 0.6 V, attributed to the reduction of EC, lithium intercalation, and lithium deintercalation at the graphite electrode surface. The reduction peak corresponding to EC disappeared in further cycles because the SEI layer on the graphite electrode blocked the further decomposition of the solvent. The electrolytes containing NI was inferred to form a stable SEI layer. Figure 20 (c) shows that E_DM 4 displayed a broad intense reduction peak between 2.0 V and 1.0 V that was present during all cycles tested. This deposition peak was attributed to the irreversible reduction of DM. Furthermore, the oxidation peak corresponding to lithium deintercalation was not observed because the E_DM 4 did not form an adequate SEI layer on the graphite electrode during the first reduction cycle. These features mainly resulted from the irreversible reductive decomposition of DM at the electrode surface. The LSV and CV results indicated that NI prevented the decomposition of the electrolytes and supported the formation of a stable SEI layer on the graphite electrode.

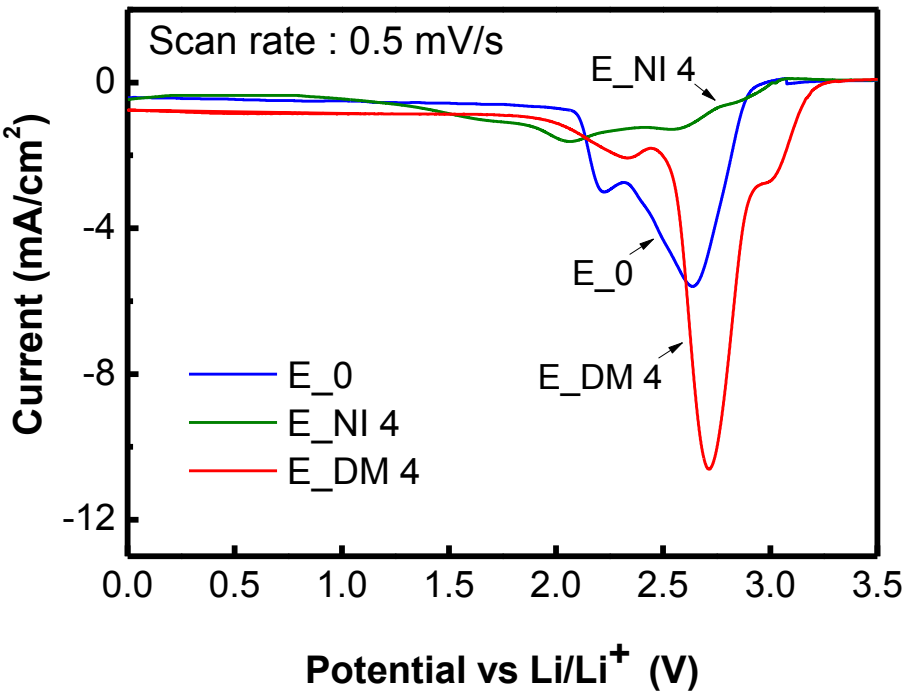

Figure 19. LSV of the electrolytes on a Pt disk electrode; E_0, E_NI 4, and E_DM 4

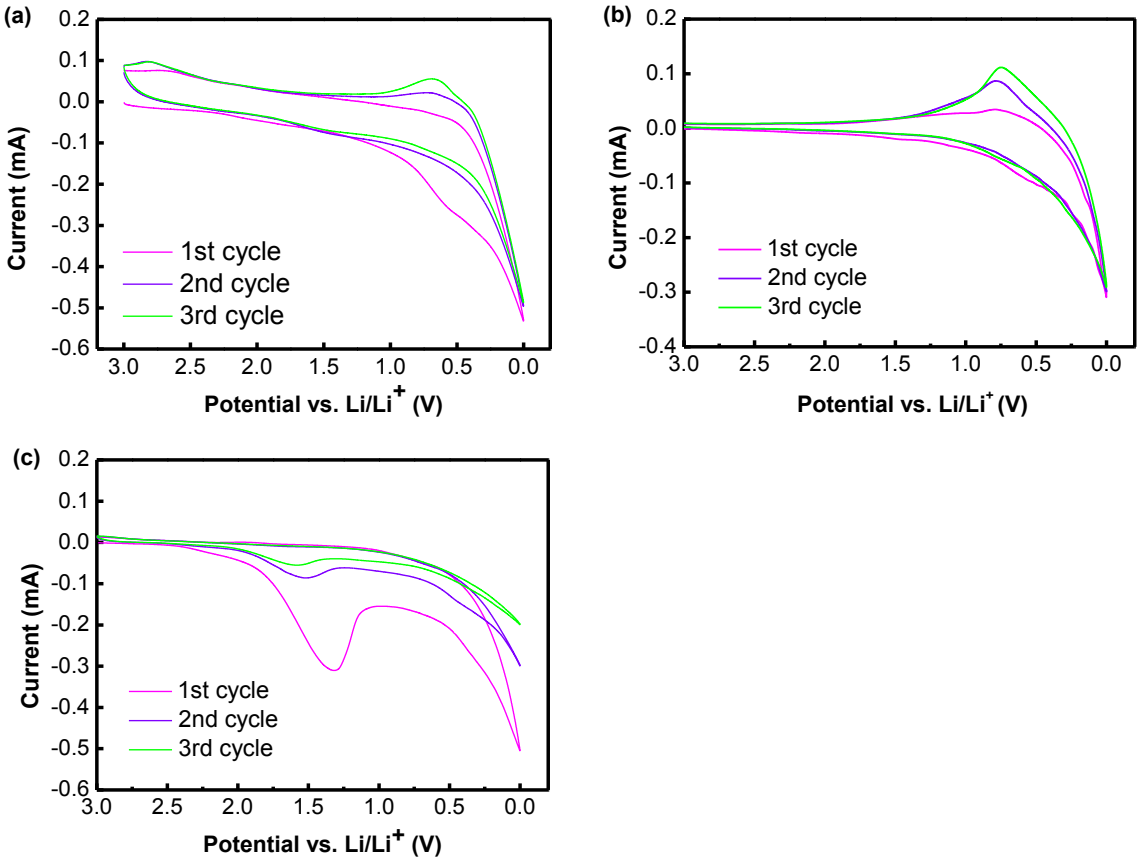

Figure 20. CV of the electrolytes on a graphite electrode; (a) E_0, (b) E_NI 4 and (c) E_DM 4

3.5. Single full cell performance test

3.5.1. Initial charge-discharge test

Effect of the NI on the graphite/$LiCoO_2$ SFC performance is confirmed by comparing E_0 and E_NI containing various amounts of the NI. The Figure 21 illustrated the initial charge-discharge profiles. All of the initial discharge curves indicated the irreversible capacity loss, which is contributed to the charge consumption at the graphite anode. In other word, this loss is related to formation of SEI layer on the graphite electrode at first cycle. The initial columbic efficiency of the full cells is found to decrease with the increasing amount of the NI. Furthermore, comparing with the E_0 and the E_NI indicated more enhanced initial discharge capacity except E_NI 16. The results listed in Table 6 shows that the coulomb efficiency of E_NI 4 was the highest value, 2.42 mAh with less than that of the E_0. In the work for the design of electrolytes, almost researchers have focused on designing the high ion conductivity electrolytes, accompanied with a low resistance SEI layer because these two factors affect to LIB performances [26]. The above mentioned results show that ion conductivity of E_NI is higher than that of E_0. If these results are only determined by ion conductivity value, it would be critical factor of decisive initial charge-discharge property. However, although the ion conductivity of E_NI 8 examined here has a higher value than that of the E_NI 4, initial capacity of E_NI 8

appeared the inversely proportional result. Hence, the ion conductivity is not a crucial factor to determine the initial performance of the full cell at least in this ion conductivity range and in this system. Therefore, the initial cell performance is significantly influenced by the stability of the SEI layer. As a result, it is inferred that one of the most stable SEI layer was produced in E_NI 4.

The formation of an SEI layer during the initial charging process could be monitored using the differential capacity (dQ/dV) curve data. Figure 23 shows the dQ/dV plots of the SFCs during the 1st and 2nd cycles. As shown in Figure 22, all curves displayed an initial decomposition peak during the first cycle that vanished during the second cycle. These properties were common to all SEI layer formation. The SEI layer formed during the initial charge, and this film prevented further decomposition of the electrolytes during subsequent charge processes. Furthermore, the E_DM 4 show peak in the 1.5–2.0 V range, which is not seen for the E_NI 4. This Peak is associated with a component in the DM additive that is reduced (and apparently decomposed) early on the initial charge process, which the prior reduction of the DM does not prevent solvent reduction on the graphite anode. This result suggests that imidazolium-based zwitterion is enhanced the electrochemical stability by introduction of nitrile group. The nitrile group includes strongly electron-withdrawing groups. This functional group can change the electron distribution over the whole zwitterion molecular system. Accordingly, NI zwitterion has a symmetrical structure, so that charge is uniformly

distributed throughout the nitrile functional group which can improve the electrochemical stability. As shown in Figure 23, increasing the NI content gradually shifted the initial decomposition peak toward higher voltages. This movement could be explained in terms of an electrochemical reaction on the graphite electrode. Jung [27] described the initial events involved in electrolytes decomposition on graphite surfaces, illustrating that the initial decomposition peak of the dQ/dV curve was shifted toward higher potentials as the BF_4^- anion content increased due to the adsorption of BF_4^- anions. Moreover, it has been reported that zwitterionic surfactant is electrochemically adsorbed on the electrode, and at low bulk surfactant concentrations, it corresponds to the formation of a film of adsorbed molecules on the electrode surface [28]. It was, therefore, inferred that the NI electrochemically adsorbed onto the graphite surface during the aging process, and these reactions modified the electrode surfaces.

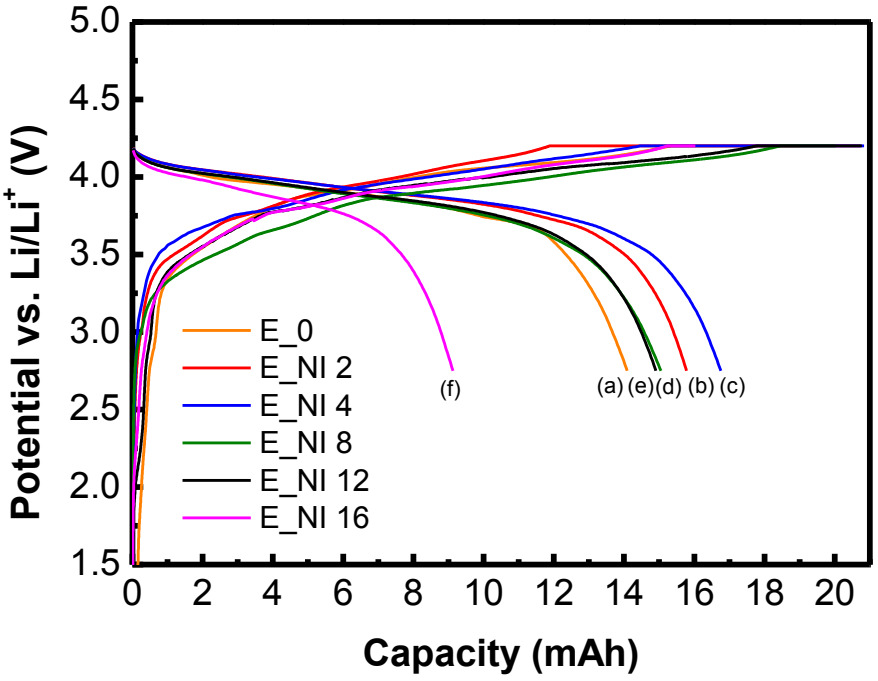

Figure 21. Battery performance of charge and discharge profiles of graphite/$LiCoO_2$ single full cell using E_0 and E_NI containing various amounts of the NI, obtained from first cycle: (a) E_0 (b) E_NI 2 (c) E_NI 4 (d) E_NI 8 (e) E_NI 12 (f) E_NI 16

Table 8. Discharge capacities and coulombic efficiencies of the E_0 and E_NI electrolytes, obtained from the first cycle.

Sample	1st cycle capacity (mAh)		Columbic efficiency (%)[a]
	Charge	Discharge	
E_0	18.99	14.34	75
E_NI 2	20.73	15.78	76
E_NI 4	20.84	16.76	80
E_NI 8	20.02	15.40	75
E_NI 12	20.76	14.90	72
E_NI 16	16.03	9.13	56

Columbic efficiency [a] **: *(Discharge capacity/charge capacity)×100***

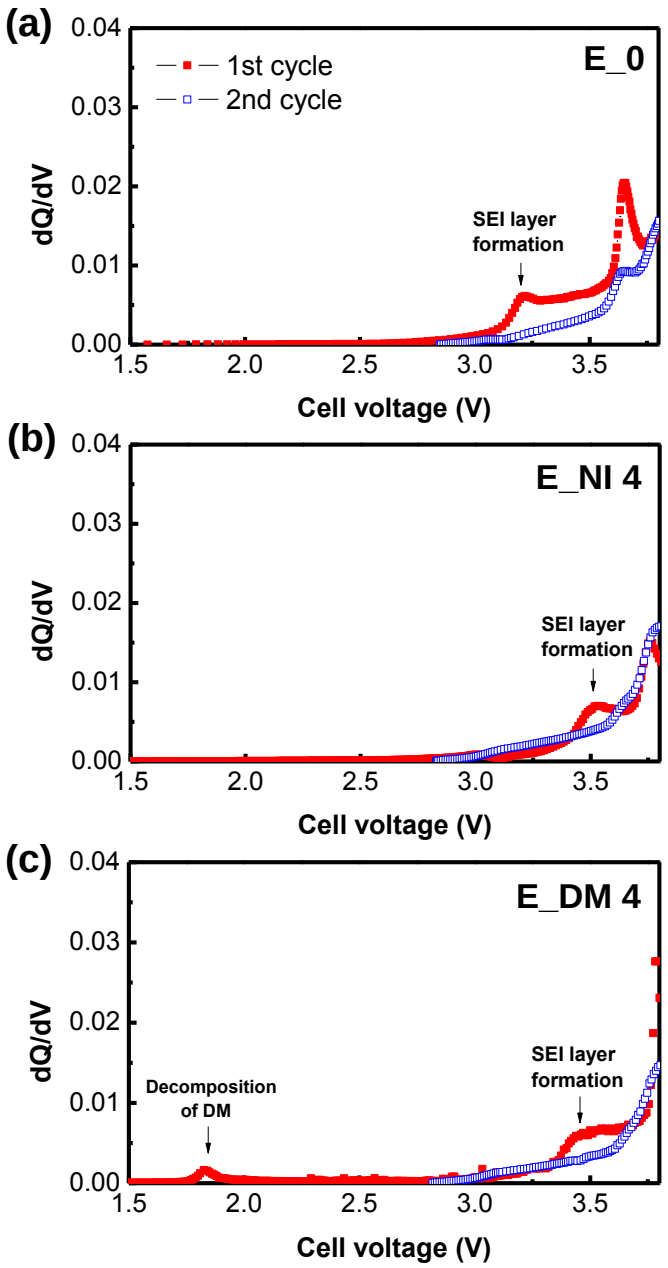

Figure 22. The differential capacity (dQ/dV) plots graph of the single full cells at 1st and 2nd cycle: (a) E_0 (b) E_NI 4 (c) E_DM 4 the arrows indicate the location of the initial decomposition peaks, respectively

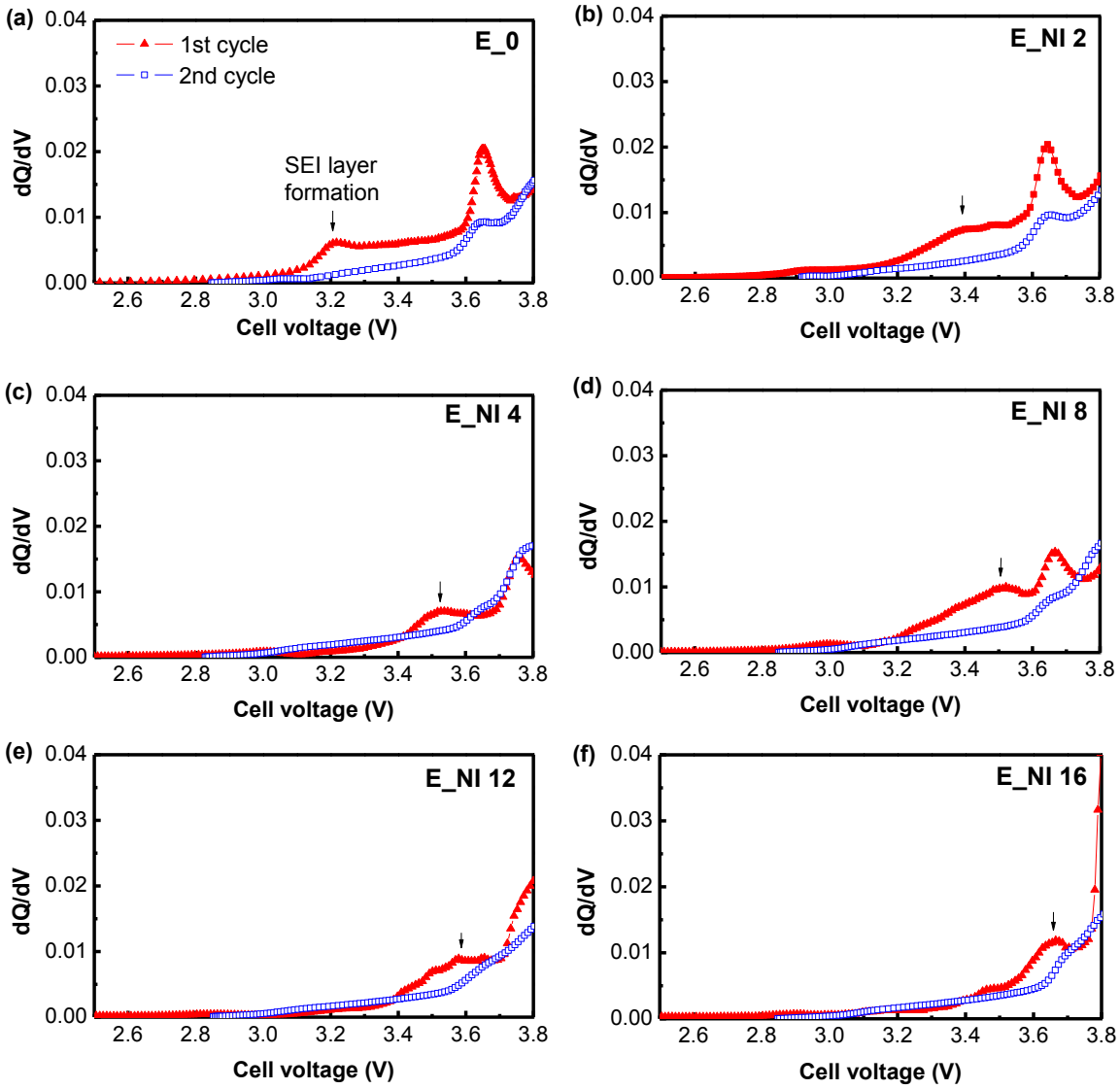

Figure 23. The differential capacity (dQ/dV) plots graph of the single full cells at 1st and 2nd cycle: (a) E_0 (b) E_NI 2 (c) E_NI 4 (d) E_NI 8 (e) E_NI 12 (f) E_NI 16; the arrows indicate the location of the initial decomposition peaks, respectively

3.5.2. Electrochemical Impedance Spectroscopy (EIS) analysis

In order to find the crucial factor about above initial charge-discharge and cell performance, EIS analysis is required. Using EIS analysis can elucidate the resistive components and the mechanism of enhancement of the cell performance. Reasonable AC impedance data may be obtained from SFCs fully charged to 4.2 V because the impedance of an SFC with a low capacity is generally very sensitive to the state of the charge. Figure 24 shows the nyquist plots of SFCs. All plots were composed of overlapping semicircles between the high and middle frequency regions and a straight line at low frequencies. These plots could be described in terms of three resistances, the bulk resistance (R_b) at high frequencies, the SEI layer resistance (R_{SEI}) corresponding to the semi-circular response at high frequencies, and the charge transfer resistance (R_{ct}) corresponding to the semi-circular response at medium to low frequencies. These single full cell impedance data was mainly affected by the graphite anode. Moreover, the main differences were observed in the mid-frequency semicircles of the EIS data, which indicated differences in the graphite–electrolytes interface, that is, in the SEI formed in various electrolytes. The order of interfacial resistance of these electrolytes is as follows: E_NI 16 > E_0 > E_NI 8 > E_NI 12 > E_NI 2 > E_NI 4. This result is shown that the NI containing electrolytes exhibits much lower interfacial resistance than the E_0. Especially, R_{SEI} and R_{ct} of E_NI 4, both of which represented the interfacial

resistance, yielded the lowest values. Interfacial resistance is associated with the SEI layer properties; therefore, E_NI 4 appeared to form low-resistance and stable SEI layer on the graphite surface; however, all resistance values (R_b, R_{SEI}, and R_{ct}) in E_NI 16 were found to be higher than those of E_0. These results were attributed to an increase the viscosity of the electrolytes and increase the interfacial resistance of the SEI layer [29]. As a result, the resistance to Li^+ ion transport through the SEI layer deceased in E_NI 2, E_NI 4, E_NI 8 and E_NI 12.

In case of the E_NI 4 results, it is necessary to understand of the SEI layer formation process. Accordingly, the main cause of enhancing SEI layer property can be verified by above mentioned differential capacity and LSV data. As shown in differential capacity data, shifting a reduction peak can be explained by electrochemical absorption of the NI. Thus, indicating low current intensity of E_NI 4 can be elucidated by effect of electrochemical absorption of NI on the electrode surface as shown LSV reduction data. Therefore, these results suggest that the adsorbed NI prevented decomposition of the electrolytes at the electrode surface during the initial charge process so that this process supported the formation of a stable SEI layer with a low interfacial resistance, thereby improving the initial capacity, rate discharge capability and cyclic performance.

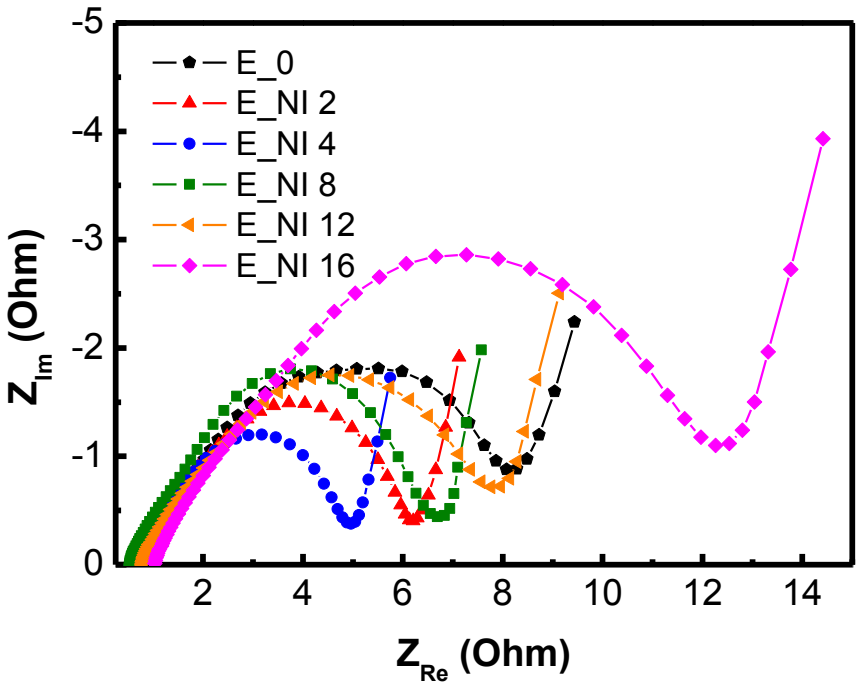

Figure 24. EIS data of the single full cells at 4.2 V after formation in a frequency range from 200 kHz to 10

3.5.2. C-rate and cyclic performance

In order to evaluate the effects of NI addition on the single full cell, charge–discharge tests were performed. These processes are performed at 20 ℃ at different discharge rates of 0.2 C, 0.5 C, 1.0 C and 2.0 C, respectively. Figure 25 shows the C-rate performance of E_0 and E_NI containing various amounts of the NI. All of the electrolytes indicated that discharge capacity was decreased with increasing C-rate. It is explained by the electric polarization because to the increase of the IR drop [30]. Moreover, although they have differential initial columbic efficiency, samples exhibit similar discharge performance at low discharge rate. However, with gradually increased the C-rate, the effect of NI on rate performance becomes more noticeable. Especially, the E_NI 4 can still deliver a capacity of 14.8 mAh at 2.0 C, showing an excellent high rate discharge capability. The E_NI 4 showed the capacity retention at 89.0% of the capacity at the discharge rate of 2.0 C. The rate performance of cell with the E_0, E_NI 2, E_NI 8 and the E_NI 12 were 83.5%, 88.4%, 87.4% and 87.1% of capacity retention at 2.0 C, respectively. The order of capacity retention of these electrolytes at 2.0 C is as follows: E_NI 4 > E_NI 2 E_NI 8 > E_NI 12> E_0 > E_NI 16. This result is shown that the NI containing electrolytes exhibits much higher rate capability than the E_0. The high rate capability arising from the high electronic conductivity induced by the thick SEI layer formed on electrode surface and high ion conductivity of the electrolyte. Thus, since electrolyte containing NI is enhancement of ion

conductivity as well as formation of low resistance and stable SEI layer, these improvements brought high rate capability.

The cyclic performances were also evaluated with the electrolytes. As shown in Figure 26, the initial discharge capacities of the single full cells containing the E_NI 2, E_NI 4, E_NI 8, E_NI 12 and E_0 at 1.0 C rate were maintained without the noticeable fluctuating to 100 cycles. On the contrary, the cell capacity of containing the E_NI 16 is rapidly reduced during the cycles. The noticeable thing that the cell capacity of the battery containing E_NI 2, E_NI 4, E_NI 8 and E_NI 12 exhibited better cyclic performance at 1.0 C than that containing the E_0. However, compared their cell capacity, there are a little different in the single full cell system. These phenomena correspond with above C-rate capability results indicating a little gap of capacity at 1.0 C rate.

These high cyclic performances were caused by enhanced SEI layer properties. In EIS results, the interfacial resistance (R_{SEI} and R_{ct}) was increased with amount of the NI contents. Increased interfacial resistance is strongly depends on thickness and resistance of the SEI layer. Therefore, in these results, it can prove that the E_NI, except E_NI 16, indicating best cyclic performance formed low-resistance and stable SEI layer on the graphite surface.

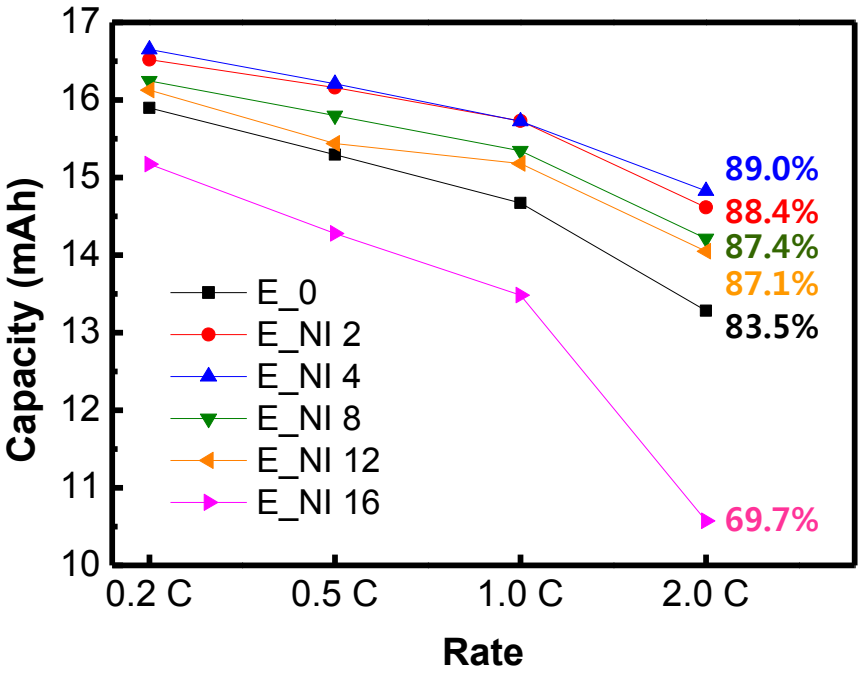

Figure 25. C-rate dependency of the discharge capacities of the graphite/$LiCoO_2$ cell at different discharge rates of 0.2 C, 0.5 C, 1.0 C and 2.0 C

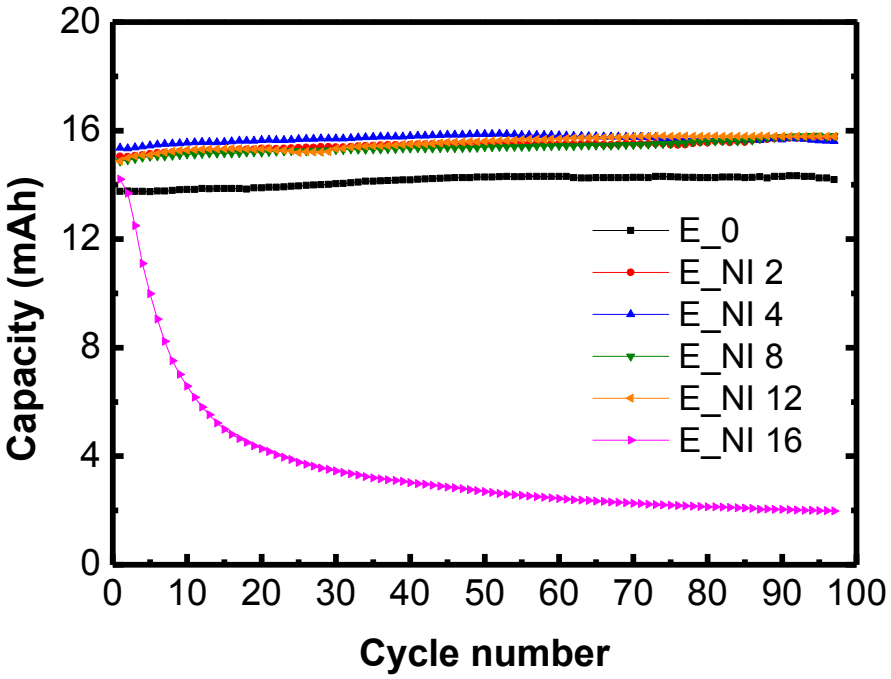

Figure 26. Cyclic performance for the graphite/$LiCoO_2$ cell at 1.0 C rate

4. Conclusions

In this study, In order to find out effect of the nitrile-functionaliuzed zwitterion (NI) was synthesized and added into organic carbonated electrolytes to application for LIB. Some of the results are as the follow.

1. The nitrile-functionalized zwitterion (NI) is synthesized to using of LIB electrolytes. The results of the ^{1}H−NMR and EA confirmed that Pre-NI is successfully conversion of the NI. Moreover, the FAB−MS is excellent in giving the correct molecular formula.

2. The methyl-functionalized zwitterion (DM) is synthesized using for control group of NI. The successfully conversion of the DM structures was verified by ^{1}H−NMR and EA. Moreover, the FAB−MS can identify of the correct molecular formula.

3. The thermal properties of the NI and DM were examined by TGA and DSC, respectively. From these results, it is indicated that the DSC curve of NI showed T_g and overwrapped between T_m and decomposition point. Additionally, TGA curve of the NI present two distinct stability regions. The

initial weight loss of the NI occurred in around 24% in the temperature range of between 220 ℃ and 250 ℃, which is likely attributed to the nitrile functional group. Consequently, the NI exhibited high thermal stability so that LIB electrolytes using this zwitterion would be safe even at high thermal environment.

4. The room temperature (20 ℃) ion conductivity of electrolytes which incorporated with various amount of two kinds of zwitterion are estimated. The ion conductivity gradually increased with increasing NI content. The ion conductivity of E_NI 8 reached a maximum value of 7.64 mS/cm; however, as the NI concentration exceeded that in E_NI 8, the ion conductivity rapidly decreased. This was explained by assuming that the functionalized nitrile groups cooperated with the sulfonate groups in dissociating Li^+ ions from the salts. The interaction between Li^+ ions and zwitterion was investigated by FT−IR spectroscopy. In this results, it is founds that the NI that Li^+ ion interacts with both nitrile group and sulfonate group, thereby the NI facilitates dissociation of lithium salt.

5. LSV show that comparing the E_NI 4 with the E_0, the E_NI 4 has the lower reduction current than the E_0. These low-intensity current mean that

electrolytes reduced the reduction decomposition on the electrode surface. In other words, NI prevented the electrolytes decomposition on the electrode surface. Therefore, LSV indicated that The NI was inferred to prevent electrolyte decomposition on the electrode surface. Moreover, effect of the NI on the compatibility between the graphite anode and the electrolytes is investigated by cyclic voltammetry (CV) testing. These results show that E_NI 4 can form a stable SEI layer on the graphite electrode. The LSV and CV results indicated that NI prevented the decomposition of the electrolytes and supported the formation of a stable SEI layer on the graphite electrode.

6. Effect of NI on the SFC performance is confirmed by comparing E_0 and E_NI with various amounts of the NI. Comparing with the E_0, the E_NI indicated more enhanced initial discharge capacity except E_NI 16. Furthermore, examining the differential capacity (dQ/dV) curve, it can be found that the shifting initial decomposition peak to high voltage is caused by modified graphite surface due to electrochemical absorption of NI on the electrode surface.

7. Using EIS analysis can elucidate the resistive components and the mechanism of enhancement of the cell performance. The order of interfacial resistance of

these electrolytes is as follows: E_NI 16 > E_0 > E_NI 8 > E_NI 12 > E_NI 2 > E_NI 4. This result is shown that the NI containing electrolytes exhibits much lower interfacial resistance than the E_0. Especially, R_{SEI} and R_{ct} of E_NI 4, both of which represented the interfacial resistance, yielded the lowest values. In case of E_NI 4, interfacial resistance, such as R_{SEI} and R_{ct}, is indicated the lowest value. As a result, the resistance to Li^+ ion transport through the SEI layer deceased in E_NI 2, E_NI 4, E_NI 8 and E_NI 12.

8. In order to evaluate the effects of NI on the single full cell, charge–discharge tests are performed at 20 ℃ at different discharge rates of 0.2 C, 0.5 C, 1.0 C and 2.0 C, respectively. The E_NI 4 can still deliver the capacity of 14.8 mAh at 2.0 C, showing an excellent high rate discharge capability. The order of capacity retention of these electrolytes at 2.0 C is as follows: E_NI 4 > E_NI 2 > E_NI 8 > E_NI 12> E_0 > E_NI 16. This result is shown that the NI containing electrolytes exhibits much higher rate capability than the E_0.

9. The cyclic performances were evaluated with the electrolytes. The initial discharge capacities of the single full cells containing the E_NI 2, E_NI 4, E_NI 8, E_NI 12 and E_0 at 1.0 C rate were maintained without the noticeable fluctuating to 100 cycles. On the contrary, the capacity of containing E_NI 16

is rapidly reduced during the cycles. The noticeable thing that the cell capacity of the single full cells containing E_NI 2, E_NI 4, E_NI 8 and E_NI 12 exhibited better cyclic performance at 1.0 C than that containing the E_0.

In conclusion, NI with enhanced electrochemical stability was successfully synthesized, and the NI as an additive of the electrolytes plays an importance role in the stabilization of SEI layer on electrode and enhancement of ion conductivity, which can be a crucial factor to improve initial capacity and cyclic performance.

4. Reference

[1] Lithium Battery Energy Storage (LIBES) Publication, Technological Reserch Association, Tokyo, 1994.

[2] G.A. Narzri, G. Pistoia, 2003, Science and Technology of Lithium Batteries, Kluwer Academic Publishers, Boston, pp. 3–41.

[3] K. Xu, Chem. Rev. 104 (2004) 4303–4417.

[4] C. Jung, Solid State Ionics, 179 (2008) 1717–1720.

[5] W.H. Meyer, Adv. Mater. 10 (1998) 439–448.

[6] M. Armand, F. Endres, D. R. MacFarlane, H. Ohno, B. Scrosati, Nat. Mater. 8 (2009) 621–629.

[7] A. Lewandowski, A. Swiderska-Mocek, J. Power Sources 194 (2009) 601–609.

[8] S.-Y. Lee, H.H. Yong, Y.J. Lee, S.K., S. Ahn, Phys. Chem. B 109 (2005) 13663–13667.

[9] M. Yoshizawa, M. Hirao, K. Ito-Akita, H. Ohno, Mater. Chem. 11 (2001) 1057–1062.

[10] A. Narita, W. Shibayama, H. Ohno, J. Mater. Chem. 16 (2006), 1475–1482.

[11] C. Tiyapiboonchaiya, J.M. Pringle, J. Sun, N. Byrne, P.C. Howlett, D.R. MacFarlane,

M. Forsyth, Nat. Mater. 3 (2004) 29–32.

[12] D.Q. Nguyen, H.W. Bae, E.H. Jeon, J.S. Lee, M. Cheong, H. Kim, H.S. Kim, H. Lee, J. Power Sources 183 (2008) 303–309.

[13] H. Kim, D.Q. Nguyen, H.W. Bae, J.S. Lee, B.W. Cho, H.S. Kim, M. Cheong, H. Lee, Electrochem. Commun. 10 (2008) 1761–1764

[14] M. Yoshizawa-Fujita, T. Tamura, Y. Takeoka, M. Rikukawa, Electrochem. Commun. 47 (2011) 2345–2347.

[15] H. Tsutsumi, A. Matsuo, K. Takase, S. Doi, A. Hisanaga, K. Onimura, T. Oishi, J. Power Sources 90 (2000) 33–38.

[16] Z. Wang, , B. Huang, R. Xue, X. Huang, L. Chen, Solid State Ionics 121 (1999) 141–156.

[17] M. Egashira, S. Okada, J.-I. Yamaki, D.A. Dri, F. Bonadies, B. Scrosati, J. Power Sources 138 (2004) 240–244.

[18] L. Zhao, J.-i. Yamaki, M. Egashira, J. Power Sources 174 (2007) 352–358.

[19] P. Isken, C. Dippel, R. Schmitz, R.W. Schmitz, M. Kunze, S. Passerini, M. Winter, A.

Lex-Balducci, Electrochim. Acta 56 (2011) 7530–7535.

[20] M.Z. Kufian, S.R. Majid, Electrochim. Acta 16 (2010) 409–416.

[21] Z.H. Li, Q.L. Xi, L.L. Liu, G.T. Lei, Q.Z. Xiao, D.S. Gao, X.D. Zhou. Electrochim. Acta 56 (2010) 804–809.

[22] B. Garcia, S. Lavallee, G. Perron, C. Michot, M. Armand, Electrochim. Acta 49 (2004) 4583–4588.

[23] M. Egashira, S. Okada, J. Yamaki, N. Yoshimoto, and M. Morita, Electrochim. Acta 50 (2005) 3708–3712.

[24] F. Xu, B. Beak, C. Jung, J Solid State Electrochem. 16 (2012) 305–311.

[25] K. Abe, H. Yoshitake, T. Kitakura, T. Hattori, H. Wang, M. Yoshio, Electrochim. Acta 49 (2004) 4613–4622.

[26] K. Xu, S. Zhang, J.L. Allen, T.R. Jow, J. Electrochem. Soc. 150 (2003) A170–A175.

[27] C. Jung, Solid State Ionics 179 (2008) 1717–1720.

[28] E. Cholewa, I. Burgess, J. Kunze, J. Lipkowski, J. Solid State Electrochem. 8 (2004) 693–705.

[29] J. Liu, Z. Chen, S. Busking, I. Belharouak, K. Amine, J. Power Sources 174 (2007) 852–855.

[30] O.K. Park, Y. Cho, S. Lee, H.-C. Yoo, H.-K. Song, J. Cho, Energy Environ. Sci. 4 (2011) 1621–1633.

국문 초록

본 연구에서는 니트릴 관능기를 포함하는 양쪽성 이온이 첨가된 유기 카보네이트계 전해질을 리튬이온전지용 전해질로 사용 시, 이온 전도도의 향상과 전극 계면에 안정한 Solid electrolyte interface layer (SEI layer)을 형성 함으로써 리튬이온전지의 초기 방전용량 증가, C-rate 특성 향상과 장기 안정성이 향상 됨을 확인하였다. 이러한 양쪽성이온에서 니트릴 관능기의 효과를 확인하기 위해 니트릴 관능기를 갖는 1-(propane nitrile)-2-methylimidazolium-3-(propyl sulfonate) (NI)와 메틸기를 포함하는 1,2-dimethylimidazolium-3-(propyl sulfonate) (DM)을 합성하여 비교 실험을 실시하였다. 두 양쪽성 이온의 합성 여부를 확인하기 위해, 핵자기 공명(^{1}H−NMR), 원소분(EA)과 질량분석(FAB−MS)을 실시하였다. 이렇게 합성된 두 양쪽성 이온은 1 M의 $LiPF_6$리튬염과 유기 카보네이트계 전해질인 에틸렌 카보네이트(ethylene carbonate EC): 디에틸렌 카보네이트(diethylene carbonate DEC) (3:7 V/V) 구성되어 있는 전해질에 0.02 M, 0.04 M, 0.08 M, 0.12 M, 0.16 M의 다양한 함량으로 첨가(두 양쪽성 이온을 포함하는 전

해질과 포함하지 않는 전해질을 각각 E_NI, E_DM와 E_0로 명명하였다)하여 이온 전도도 측정 및 전극 계면에서 분해 반응을 평가하였다. 그리고 흑연과 $LiCoO_2$ 전극으로 구성된 리튬이차전지를 제조하여 NI가 0.02 M, 0.04 M, 0.08 M, 0.12 M, 0.16 M 함량 별로 첨가된 전해질의 초기 충·방전 용량, C-rate 특성 및 장기 수명 특성 등의 리튬이온전지의 성능을 비교 평가하였다.

먼저 상온(20 °C)에서 두 양쪽성 이온의 함량에 따른 이온 전도도 측정 결과, E_DM의 경우에는 모든 함량에서 E_0 보다 낮은 이온 전도도를 나타낸 반면, 일정 함량의 NI (0.02 M, 0.04 M, 0.08 M, 0.12 M)를 포함하는 전해질의 경우, E_0 보다 이온 전도도가 향상됨을 확인하였다. 특히 NI가 0.08 M 포함된 전해질의 경우 이온 전도도가 7.64 mS/cm로 가장 큰 값을 나타내었다. 그리고 적외선 분광법(FT−IR)을 통해서는 리튬 이온과 양쪽성이온 간의 상호 작용력을 확인하였다. 그 결과, NI의 설포네이트기와 니트릴기가 동시에 리튬 이온과 강한 상호작용을 한다는 것을 확인하였다. 이러한 리튬 이온과의 강한 상호작용력은 리튬염의 해리도를 향상시킴으로써 전해질의 점도 감소 및 리튬 이온의 이동성을 증가시킴으로써 전해질의 이온 전도도가 향상 되었다고 볼 수 있었다.

전극 계면에서의 전해질의 분해반응을 확인하기 위해 선형주사 전압 전류법(linear sweep voltammetry, LSV)과 순환주사 전압 전류법(cyclic voltammetry, CV)를 실시하였다. LSV를 통해서는 니트릴기를 양쪽성 이온에 도입함으로써 전기화학적 안정성이 향상 됨을 확인하였다. 또한 전극계면에서의 전해질의 분해가 E_NI가 E_0에 비해 큰 폭으로 감소함을 확인함으로써, NI가 전극 계면에서 전해질 분해를 보호함을 확인하였다. CV를 통해서는 흑연 전극 계면에 E_NI 4의 경우 안정한 SEI layer가 형성되는 반면, E_DM 4는 계속적인 양쪽성 이온의 분해반응으로 인하여 안정한 SEI layer를 형성하지 못하여 리튬 이온의 탈·삽입이 원활하지 못함을 확인하였다.

NI의 함량에 따른 전지 성능 평가 결과, 일정함량의 NI (0.02 M, 0.04 M, 0.08 M, 0.12 M)가 포함된 전해질을 주입한 전지에서 E_0를 주입한 전지보다 초기 충·방전 용량이 증가하였으며, C-rate 특성 및 장기 안정성 또한 향상 됨을 확인하였다. 특히 NI가 0.04 M 첨가된 전해질의 경우 16.76 mAh의 초기 방전 용량과 80%의 columbic efficiency로 가장 우수하게 나타내었다. 그리고 C-rate 특성 평가에서도 높은 C-rate에서도 가장 높은 방전 용량과 용량 유지율를 나타

내었으며, 장기 수명 특성 평가에서 또한 100 싸이클 동안 높은 용량을 유지하며 안정하게 충·방전을 하는 것을 확인하였다.

전기화학적 임피던스 분광법을 통해서는 전지 내부저항을 측정하여 전지의 계면저항을 비교하였다. 비교 결과, E_0를 주입한 전지보다 우수한 전지 성능을 나타낸 일정 함량의 NI (0.02 M, 0.04 M, 0.08 M, 0.12 M)가 첨가된 전해질을 주입한 전지의 경우, E_0보다 낮은 계면 저항을 나타냄을 확인하였으며, 가장 우수한 성능을 나타낸 NI가 0.04 M 첨가된 전해질을 주입한 전지의 경우, 가장 낮은 계면저항을 나타내었다. 이러한 낮은 계면저항은 전극 계면에 낮은 저항의 안정한 SEI layer가 형성됨을 의미한다. 이러한 안정한 SEI layer가 형성된 원인은 NI가 에이징(aging) 과정 중 전극 계면에 안정하게 흡착 함으로써 초기 충·방전 시에 나타나는 전극 계면에서의 전해질 분해를 보호하여 낮은 저항의 안정한 SEI layer가 형성되었다는 것을 LSV 결과와 초기 충전 과정의 미분용량 (differential capacity dq/dv) 결과를 바탕으로 해석하였다.

위의 실험들을 통해, 전지 성능의 향상이 이온 전도도의 향상과 및 전극 계면의 안정한 SEI layer의 형성에 모두 기인한 것임을 확인 하였다. 하지만

향상된 이온 전도도의 효과보다 SEI layer의 안정성 향상이 전지 성능 향상에 더 크게 기여함을 실험 결과들을 통해 확인하였다. 위의 결과를 통해, 새롭게 합성한 니트릴 관능기를 포함하는 양쪽성이온을 전해질에 첨가 시, 이온 전도도의 향상과 안정한 SEI layer의 형성을 통해 전지 성능이 향상 됨을 확인함으로써, NI가 리튬이차전지 전해질의 첨가제로써 활용 가능성이 있음을 확인하였다.

감사의 글

2년간의 길고도 짧았던 석사과정을 마치고 이제 다음 단계로 도약하고자 합니다.

먼저 2년 동안 좋은 연구환경을 만들어 주시고 많은 지도와 가르침을 통해 논문이 완성되기까지 큰 도움을 주신 곽승엽 교수님께 진심으로 감사를 드리며 바쁘신 와중에도 논문 심사와 지도를 해주신 장지영 교수님과 안철희 교수님, 그리고 큰 어려움 없이 연구를 진행할 수 있도록 도와주신 한국에너지기술연구원 전재덕 박사님께도 감사의 말을 전하고 싶습니다.

석사과정 동안 힘들고 어려운 일이 있어도 이겨낼 수 있었던 것은 항상 힘이 되어주고 격려와 조언을 해준 연구실 식구들이 함께 하였기 때문이 아닐까 싶습니다. 바쁘신 와중에도 귀한 시간 쪼개어 졸업 논문을 도와주신 병용이형과 성학이형, 컴퓨터를 잘 모르던 저에게 기초를 잘 가르쳐 주신 형구형, 에너지팀 팀장으로서 항상 옆에서 조언을 아끼지 않으셨던 현중이형, 처음 연구를 시작 할 때 정말 많은 도움을 주셨던 성용이형, 졸업 논문을 처음부터 끝까지 잘 지도해주신 우혁이형, 나이는 비록 어리지만 선배로서 많을 것을 도와준 지훈이, 2년 동안 힘들고 지칠 때마다 옆에서 항상 힘이 되어준 믿음직하고 성실한 최고의 동기 지환이와 태선이, 오랜 기간 연구실 궂은 일도 마다 않고 도맡아 해 준 규원이, 효원이형 그리고 비록 한 학기뿐이 같이 하지 못하여 아쉽지만 항상 옆에서 성실히 도와준 준호와 민영이 모두의 도움이 없었더라면 이러한 결실을 맺을 수 없을 것이었기에 진심으로 고맙다는 말을 전하고 싶습니다.

끝으로 2년동안 아무런 탈없이 잘 마무리 할 수 있도록 지켜봐 주신 하나님께 감사 드리고 저를 지켜봐 주시고 힘이 되어준 많은 친구들과 교회 식구들 그리고 2년 동안 물심양면으로 묵묵히 지원해시고 인생의 멘토 역할을 해주신 부모님과 저의 하나뿐인 형 원진이형에게 작지만 소중한 결실로써 보답할 수 있게 되어 너무나 기쁘고, 한없이 감사하고 또 감사하다는 말을 전하고 싶으며 큰 은혜에 보답할 수 있도록 앞으로도 최선을 다하겠다는 말을 전합니다.